

# ENVIRONMENTAL RECONSTRUCTIONS FOR THE APTIAN (MID-CRETACEOUS) OF THE CARPENTARIA BASIN (NE AUSTRALIA) BY MEANS OF GEOCHEMICAL AND PALYNOLOGICAL RECORDS FROM BMR MOSSMAN-1.

## Abstract

Well BMR Mossman-1 from the Carpentaria Basin was studied for palynology, organic-carbon-isotope ( $\delta^{13}\text{C}_{\text{org}}$ ) stratigraphy and total organic carbon (TOC) content. The  $\delta^{13}\text{C}_{\text{org}}$  record was biostratigraphically calibrated in part on the basis of dinoflagellate cyst events, inferring a latest Barremian-Aptian age for the section at Mossman. Comparison of the  $\delta^{13}\text{C}_{\text{org}}$  data with time-equivalent Tethyan and Atlantic records shows identical stratigraphic changes and reveals an interval in Mossman which includes the period of the oceanic anoxic event (OAE) 1a. Although this interval corresponds with a lithologic unit comprising 1.5 m thick shale and mudstone, it does not show elevated TOC values. Palaeoenvironmental reconstructions, based on selected groups distinguished within the dinoflagellate cyst and sporomorph assemblages, indicate warmer and wetter conditions prior to this level, changing to cooler and drier conditions at the start of the presumed OAE 1a.

In the marine environment this temperature shift was coeval with a rapid rise in sea level, possibly coinciding with the development of a circum-Antarctic-Australian connection in the Early Aptian bringing cold waters to northeastern Australia. The inferred second and third order sea-level fluctuations at Mossman correspond with the observed global eustatic variations.

## 1. Introduction

During the mid-Cretaceous major changes in biogeochemical cycling, climate and evolution occurred (e.g. Hay, 1995; Erbacher et al., 1996; Mutterlose, 1998; Premoli Silva and Sliter, 1999; Leckie et al., 2002). These changes episodically led to the deposition of organic rich layers in deep marine settings, also referred to as Oceanic Anoxic Events (OAEs; Schlanger and Jenkyns, 1976; Jenkyns, 1980). One of the most profound OAEs is the Early Aptian OAE 1a, which is most conspicuous in the various marine carbon isotope records. It has been observed in  $\delta^{13}\text{C}_{\text{org}}$  and  $\delta^{13}\text{C}_{\text{carb}}$  records (e.g. Menegatti et al., 1998; Bralower et al., 1999; Jenkyns and Wilson, 1999; Jahren et al., 2001; Leckie et al., 2002; Price, 2003) and is characterised by a sharp negative  $\delta^{13}\text{C}$  excursion preceding the event, followed by an abrupt and prolonged positive  $\delta^{13}\text{C}$  excursion, and black shale deposition (e.g. Menegatti et al., 1998; Bralower et al., 1999; Leckie et al., 2002; see Figure 6). In recent years, studies of non-marine sections have shown that the sharp negative excursion followed by the abrupt and prolonged positive excursion can also be recognised in continental  $\delta^{13}\text{C}_{\text{org}}$  records (e.g. Gröcke et al., 1999; Jahren et al., 2001; Ando et al., 2002). The records on which the present knowledge on mid-Cretaceous climatic and environmental changes is mainly based are from the Tethyan realm and the Atlantic and the equatorial Pacific oceans (e.g. Arthur and Premoli Silva, 1982; Weissert et al., 1985; Premoli Silva et al., 1989; Coccioni et al., 1992; Bralower et al., 1993, 1994, 1999; Menegatti et al., 1998; Erba et al., 1999; Gröcke et al., 1999; Jenkyns and Wilson, 1999; Jahren et al., 2001; Leckie et al., 2002; De Gea et al., 2003; Price 2003). The assumption that the environmental changes at the time of OAE 1a had global impact (e.g. Sliter, 1989; Bralower et al., 1994, 1999) therefore, raises the question how these changes are reflected in shallow-marine sequences from other regions, for example from Australia.

Due to the endemic character, or even total lack of stratigraphically important fossil groups (like ammonites, belemnites, foraminifera, or nannofossils), Austral marine successions have always been difficult to correlate to the standard stratigraphic scale. In recent years, however, organic-walled dinoflagellate cysts have been successfully applied to biostratigraphically correlate sequences from different realms (e.g. Prauss, 1993; Hoedemaeker and Leereveld, 1995; Wilpshaar, 1995; Leereveld, 1997; Hoedemaeker, 1999; Torricelli, 2000). For the Barremian-Aptian in NW Australia, Oosting et al. (in prep.) established fine-stratigraphic cross hemisphere correlation by means of a selection of nine diagnostic events recognized in ammonite controlled European Tethyan and Boreal sections.

The present paper is the second in a series of integrated geochemical and palynological studies, which aim to determine the extent and nature of environmental changes during the mid-Cretaceous, with emphasis on Australian successions. It presents a palynological, organic-carbon-isotope and total-organic-carbon record for a marine latest Barremian-Aptian section from the Carpentaria Basin (NW Australia). Verification and refinement of previous biostratigraphic assessments has relied on organic walled dinoflagellate cysts (dinocysts). In addition, the Barremian-Aptian carbon isotope record is used for correlation with the most complete  $\delta^{13}\text{C}_{\text{org}}$  record currently available, that of the Italian Cismon section described by Menegatti et al. (1998). These authors recognized eight sequential isotope segments (C1 to C8), which Bralower et al. (1999) extended into the Albian by the addition of seven more segments (C9 to C15) based on Atlantic sections (see Figure 6).

A reconstruction of the adjacent terrestrial environmental conditions is accomplished by evaluating quantitative sporomorph information. Interpreted fluctuations in water-mass characteristics (like salinity, temperature and nutrient supply) are based on quantitative dinocyst data. The consequent marine-terrestrial relationship allowed recognition of the effect of relative sea-level changes on the local marine and terrestrial environmental development.

## 2. Material

### 2.1 Core and lithology

The Carpentaria Basin reflects an epi-continental sea of northeast Australia during Early Cretaceous times (Figure 1), and contains thick sequences of undisturbed Lower Cretaceous sedimentary rocks (Morgan, 1980b). Mossman-1 hole was drilled in the eastern part of the Carpentaria Basin at 16°42'S and 144°01'E by the Australian Bureau of Mineral Resources (BMR) in 1971 as part of a program to document regional stratigraphy. Approximately 180.2m of mostly Lower Cretaceous rocks were cored before intersection of a conglomerate unit obstructed further drilling. The basic lithostratigraphy of these cores was described in a report (Smart and Grimes, 1971), but little additional information has been published. The cores of BMR Mossman-1 are currently stored at Geoscience Australia (Canberra).

Three lithological units are represented by the Mossman-1 core (Figure 2; Smart and Grimes, 1971): Quaternary alluvium (0-2.4 m), the Wallumbilla Formation (2.4-74.3 m) consisting of mudstone with minor sandstone and limestone of marine origin, and the Gilbert River Formation (74.3-180.2 m). The latter was subdivided into the Coffin Hill Member (74.3-111.1 m) consisting of medium-grained clayey quartz sandstone of marine origin, and the Yappar Member (111.1-180.2 m) consisting of coarse to medium-grained clayey quartz-sandstone presumed to be largely of terrestrial origin. Within this member several thin intervals with pebble conglomerate occur e.g., at 123.7-125.2 m and 127.6-131.5 m (both marked by artesian groundwater flow); pebbly beds occur between 139.4-143.7 m, and a polymictic pebble conglomerate at 155.5 to

155.8 m. The Yappar Member further contains a gray shale and mudstone with trace fossils from 114.3-115.8 m (Smart and Grimes, 1971).

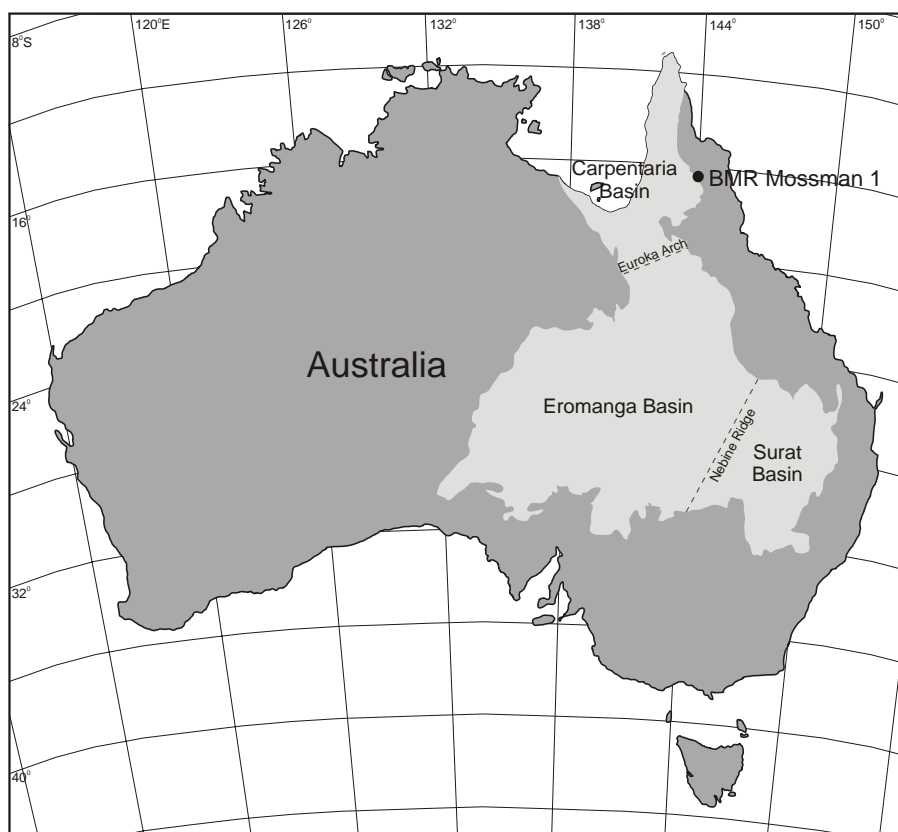


Figure 1. Map with present coastline of Australia showing location of BMR Mossman-1; shaded area outlines the Cretaceous, epicontinental Carpentaria, Eromanga and Surat basins.

In previous studies of boreholes from the Carpentaria Basin (e.g. Evans, 1966; Meyers, 1969; Burger, 1973; Smart, 1976) the Gilbert River Formation was assigned to the Neocomian, and the Wallumbilla Formation to the Aptian-Albian. Morgan (1980b) summarized in detail the lithostratigraphic framework and palynological zonation of the Early and middle Cretaceous system of Australia, and interpreted the data for each basin in terms of eustatic sea-level variations. For the Carpentaria Basin he proposed several successive transgressive-regressive cycles to explain the lithostratigraphic architecture. The Yappar Member was considered, in general, to represent the start of a Neocomian transgression with rising base level reflected by widespread fluvial aggradation in the basin. The next transgression considered as latest Neocomian in age, was thought to be represented by the shallow marine Coffin Hill Member. This unit lies within the *Foraminisporis wonthaggiensis* sporomorph Zone, which correlates to Valanginian-basal Aptian (Helby et al., 1987). Morgan (1980b) inferred the contact with the overlying Wallumbilla Formation to be transgressive and diachronous, spanning the Neocomian into the Aptian. He assigned the lower Wallumbilla Formation to his *Odontochitina operculata* dinoflagellate zone; the middle part to the *Endoceratium turneri* zone; and the upper part to the basal *Endoceratium ludbrookiae* zone (Morgan, 1980b). Later Helby et al. (1987) incorporated these zones into their Australian Mesozoic zonation scheme and assigned them, respectively, to uppermost Barremian-middle Aptian, middle Aptian-Upper Albian and Upper Albian-Upper Cenomanian. In addition to corresponding to a dinocyst zonal boundary, the base of the Wallumbilla Formation approximates the base of the *Cyclosporidites hughesii* sporomorph Zone of Helby et al. (1987), who placed it in the Early Aptian.

Two transgressive episodes were recognized by Morgan (1980b) for the Wallumbilla Formation. This unit lies within the *Cyclosporites striatus* and the *Coptospora paradoxa* zones correlated by Helby et al. (1987) with uppermost Aptian-Lower Albian and middle Albian, respectively.

Apart from one reference to results of a palynological study, to date no direct stratigraphic assessments have been published for the Mossman well. Burger (1982, figure 3) included a single sample from Mossman (from 155.1m) in a composite section of the Carpentaria Basin. He assigned the sporomorph content of that particular sample to the boundary interval of the *Cicatricosisporites australiensis* - *Foraminisporis wonthaggiensis* sporomorph Zones corresponding to his DK2 dinocyst Zone and considered it to be of Valanginian age. In the comprehensive study summarizing previously established Australian Mesozoic palynostratigraphy, Helby et al. (1987, fig. 19) also placed the boundary between the zones with the Valanginian.

## 2.2 Samples

43 samples, each approximately 10 cm<sup>3</sup> in size, were taken from BMR Mossman-1 for geochemical and palynological analyses. The samples come from intervals between 15.32-159.05 m (Figure 2).

## 3. Methods

### 3.1 Palynology

#### *Sample processing and microscopic analysis*

Samples were processed at the Laboratory of Palaeobotany and Palynology (LPP) in Utrecht, The Netherlands, following standard palynological techniques as described by Wilpshaar and Leereveld (1994) and Wilpshaar (1995). Briefly, this procedure involves sequential digestion of samples with 30% HCL and 38% HF to remove carbonates and silicates, respectively. The residues are then sieved at 20 µm and stored in glycerine water. For each sample, aliquots of residue are mounted onto two slides with glycerine gelatine.

Quantitative analysis of the palynomorph assemblages in each sample was made in three successive steps. Firstly, 100 palynomorphs (mainly dinocysts, spores, pollen, acritarchs and acid-resistant foraminiferal linings) were randomly counted on one slide. Secondly, 200 identifiable dinocysts and 200 spores/pollen were counted in the same slide to quantify the abundance of taxa. Counting was started at the same reference position on each slide. While quantifying the assemblages, the degree of pyritisation of the palynomorphs has also been taken note of. Thirdly and lastly, both slides of each sample were scanned for the presence of additional taxa.

The taxonomy and nomenclature of dinoflagellate taxa follows the Lentin and Williams Index (Williams et al., 1998). Light photomicrographs of characteristic dinocyst taxa useful for age assessment in this study were taken from the permanent scatter mounts.

Slides and sample residues from the Mossman sequence are currently stored in the collection of the LPP.

#### *Biostratigraphy*

In order to correlate the studied interval at Mossman with the Lower Cretaceous standard timescale, the dinocyst data are compared to the ammonite calibrated dinocyst zonation schemes for the Tethyan and Boreal realms (Hoedemaeker and Leereveld, 1995; Wilpshaar, 1995; Leereveld, 1997; Hoedemaeker, 1999). Oosting et al. (in prep.) recognized nine successive dinocyst events as useful for biostratigraphic correlation of northwestern Australia. These authors reported that the dinocyst species *T. tenuiceras* first occurs in the basal Aptian *tuarkyricus*

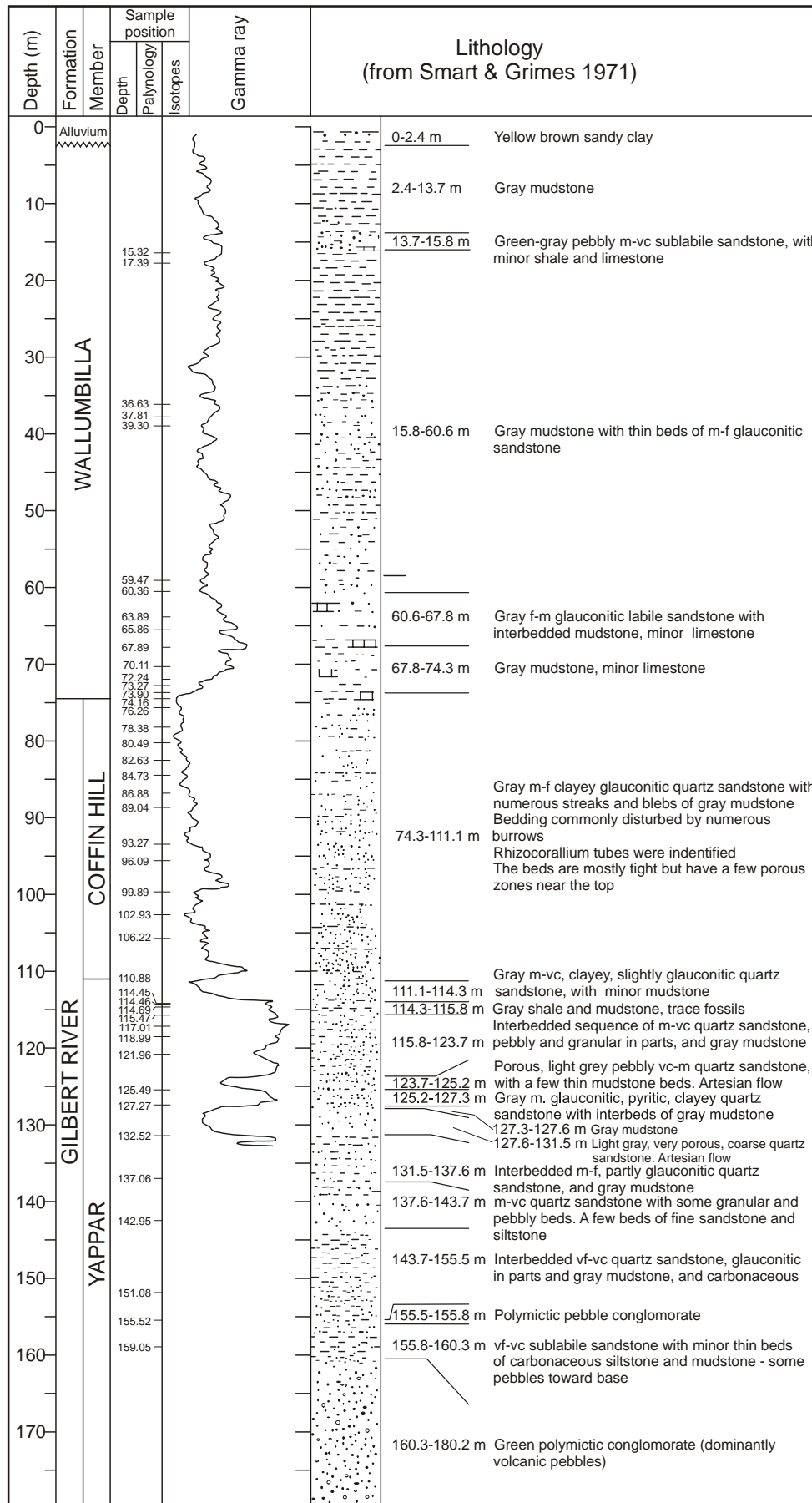


Figure 2. The stratigraphical and lithological column at BMR Mossman-1 (adapted from Smart and Grimes, 1971) with hronostratigraphic sequences (adapted from Hardenbol et al., 1998).

ammonite Chronozone in the Barremian type section (at Angles, NE France) and substantiated that this event can well be applied for cross-hemisphere correlation. In a comparison of the stable carbon isotope record from Angles and that of Cismon (NE Italy), Wissler et al. (2002) concluded that the recommended Barremian-Aptian boundary, i.e., the base of magnetic anomaly M0 (see Erba, 1996), corresponds with the base of the *tuarkyricus* ammonite Zone.

For pan-Australian comparisons, BMR Mossman-1 is correlated with the composite palynological zonation for the Lower Cretaceous developed by Helby et al. (1987).

### 3.2 Palaeoenvironmental reconstruction

#### *Dinocysts*

The quantitative composition of dinocyst assemblages is used for the reconstruction of marine environmental conditions. It provides information on water-mass features like salinity, temperature, nutrient supply and water depth (e.g. Wall et al., 1977; Davey, 1979; May, 1980; Batten, 1982; Harland, 1983; Hunt, 1987; Lister and Batten, 1988; Smelror and Leereveld, 1989). Several variables were selected which are considered to express environmental changes in the Barremian-Aptian interval of the Carpentaria Basin. These variables and their respective taxa are:

- 1) Peridinioid-Gonyaulacoid (P/G) ratio. The majority of present-day dinoflagellates has either a heterotrophic or an autotrophic life style. In general terms, of the two most abundant dinoflagellate morphologies, the peridinioid (P) type is heterotrophic and the gonyaulacoid (G) type is autotrophic. The P/G ratio therefore reflects primary productivity conditions in marine environments, i.e., being higher with increased nutrient availability.
- 2) Low salinity group. Brackish and fresh water conditions are considered to be preferred by *Muderongia* spp, *Odontochitina* spp and *Palaeoperidinium cretaceum* (e.g. Batten, 1982; Lister and Batten, 1988; Harding, 1990; Leereveld, 1995).
- 3) Littoral group. This group, characteristic of restricted and mixed near-shore environments, encompasses representatives of *Canningia*, *Circulodinium* and *Pseudoceratium/Endoceratium* (e.g. Batten, 1982; Hunt, 1987; Lister and Batten, 1988; Leereveld, 1995).
- 4) Inner neritic group. This group represents palaeoenvironments with occasional fluctuation in salinity, temperature and nutrient supply. It includes *Apteodinium* spp and *Cribroperidinium* spp (e.g. Hunt, 1987; Lister and Batten, 1988; Zevenboom et al., 1994; Leereveld, 1995).
- 5) Neritic group. This group is composed of taxa which show a relatively wide palaeoenvironmental range and partly overlaps the inner and outer neritic groups: *Spiniferites* spp, including the morphological similar *Achomosphaera* (e.g. Davey and Rogers, 1975; Harland, 1983; Brinkhuis, 1994) and *Oligosphaeridium*, including *Stiphrosphaeridium* (e.g. May, 1980; Hunt, 1987; Lister and Batten, 1988; Smelror and Leereveld, 1989).
- 6) Outer neritic group. The more open marine shelfal conditions are inferred to be reflected by *Chlamydophorella* spp and *Dingodinium cerviculum* (e.g. Smelror and Leereveld, 1989; Lutat, 1995).
- 7) Oceanic group. Characteristic of oligotrophic waters are types like *Adnatosphaeridium chonetum*, *Cannosphaeropsis/Hapsocysta*, *Endoscrinium bessebae*, *Impagidinium* spp, *Leptodinium hyalodermopsis* and *Leptodinium* spp (e.g. Wall et al., 1977; Davey, 1979; Harland, 1983).
- 8) Cool/temperate- and warm-water dinocyst groups. Comparison of global dinocyst records shows the existence of latitudinal climate zones. For the Early Cretaceous Williams et al. (1990) recognized Boreal, temperate and tropical dinocyst provincialism. In this study, dinocyst taxa consistently and frequently reported from relatively cool temperate

palaeoclimate zones (NW Europe and Canada in the northern hemisphere, and Antarctica and southern parts of Australia in the southern hemisphere) are combined in a cool/temperate group. Increased representation of this group is considered to represent fluxes of cooler sea-surface waters into the basin. Taxa involved are: *Aprobolocysta eilema*, *Aprobolocysta* sp. A, *Batioladinium jaegeri*, *B. micropodum*, *Carpodinium granulatum*, *Dingodinium cerviculum* (large forms with relatively thick walls), *Discorsia nanna*, *Heslertonia* spp, *Leptodinium hyalodermopsis*, and *Valensiella magna* (De Renéville and Raynaud, 1981; Habib and Drugg, 1987; Leereveld, 1995). Similarly, fluctuations within representation of *Endoscrinium bessebae* (compare with Below, 1981; Leereveld, 1997) are considered to reflect relative increases in sea-surface temperature.

The quantitative data of the warm and cool/temperate groups were used to reconstruct the general temperature signature.

The distribution of the palaeoenvironmental dinocyst groups is shown in Figure 3 (variables 1 to 7) and in Figure 4 (variable 8).

### *Sporomorphs*

For a palaeo-ecological and palaeoenvironmental evaluation of sporomorph types common in Australian Cretaceous successions, a wealth of information is available (see reviews by Dettmann et al., 1992; Dettmann, 1994; Douglas, 1994; Balme, 1995). The quantitative sporomorph data for Mossman were grouped according to their palaeoenvironmental significance (e.g. Dettmann, 1986; Abbink, 1998). Only spores and pollen that are well represented in most of the studied interval (taxa generally exceeding 5% of the total sporomorph assemblage of a sample) were selected. The following palaeoenvironmental groups are distinguished (Figure 5):

- 9) Podocarpaceae group (upland conifers): represented by *Podocarpidites* and *Microcachryidites*. Nowadays Podocarpaceae grow at altitude in subtropical and temperate regions of the southern hemisphere commonly at considerable distances from the shoreline (e.g. Dettmann, 1986; Dettmann et al., 1992; Abbink, 1998).
- 10) Lycopodiaceae/moss group (lowland/river, wet): represented by *Neoraistrickia* (Lycopodiaceae), *Stereisporites* (moss), and *Vitreisporites pallidus* (Caytoniales). Extant lycopsids have been reported from tropical, temperate and boreal regions in association with wet conditions (Dettmann, 1986; Abbink, 1998). Mosses have been associated with similar wet environments (Dettmann, 1986; Abbink, 1998). Although *Vitreisporites pallidus* has been associated with various palaeoenvironments (Harris, 1964; Pelzer, 1984; Van Konijnenburg-Van Cittert and Van der Burgh, 1989) they all have in common that they are associated with wet conditions (Abbink, 1998).
- 11) Osmundaceae group (lowland, warm/temperate and humid; ferns): represented by *Osmundacidites* and *Baculatisporites*. While most ferns are tropical, Osmundaceans occur in temperate environments as well (Abbink, 1998). They presumably grew on forest margins and in the understory, and they often occur together with Lycopodiaceae and mosses (Dettmann et al., 1992). However, Osmundacean ferns are considered to prefer generally drier conditions than lycopods and mosses.
- 12) Cyatheaceae group (lowland, warm/temperate and less humid; ferns): represented by *Cyathidites* and *Gleicheniidites*. Although this type of ferns grew on forest margins and in the understory like Osmundaceae (Dettmann et al., 1992), Cyatheacean ferns are interpreted to reflect less specific wet conditions (Abbink, 1998). Gleicheniaceae can even withstand full sunlight (Abbink, 1998).
- 13) Araucariaceae group (coastal, cool/temperate and dry; conifers): represented by *Araucariacites* and *Callialasporites*. Araucarian trees grew in forests nearby coastal regions (Vakhrameev, 1991; Dettmann et al., 1992) and are able to withstand extended cold and dry periods (Dettmann et al., 1992; Abbink, 1998) as well as the influence of salt wind (Abbink, 1998).

- 14) Cheirolepidaceae group (coastal, warm/temperate and dry; conifers): represented by *Classopollis/Corollina*. Cheirolepidacean shrubs are inferred to be able to withstand the continued influence of salt spray (Abbink, 1998) and drought. They are most abundant in coastal environments under relatively dry and warm conditions (Vakhrameev, 1991; Dettmann et al, 1992; Abbink, 1998), but can occur in temperate zones also (Vakhrameev, 1991).

The palynological data further enable a direct marine-terrestrial comparison (marine proportion relative to the proportion of terrestrially derived palynomorphs) and as such makes local sea-level reconstructions possible.

### 3.3 Geochemistry

Total organic carbon (TOC) was determined on all samples by combustion. Approximately 10 mg of sediment were placed into a AS200 sampler and analyzed using a Fisons Elemental Analyser NA 1500 NCS at the Department of Earth Sciences, Utrecht University. Contents were determined by standard comparison using atropine and acetanilide standards. On the basis of 3 replicate samples of F-turbidite, precision of the TOC analyses was better than 0.5%

Carbon isotope measurements were carried out on the organic carbon fraction of samples. The TOC values were used to determine the amount of powdered sample needed to generate sufficient organically-derived CO<sub>2</sub>. C-isotope measurements were conducted at Utrecht University on a Fisons Elemental Analyser NA 1500 NCS coupled to a Finnigan MAT Delta Plus isotope ratio mass spectrometer. Precision of the analyses for replicate samples and standards is better than 0.15‰. Data is reported in standard delta notation ( $\delta^{13}\text{C}$ ) versus Pee Dee Belemnite (V-PDB).

In order to constrain the type of organic carbon, selected samples (based on TOC) were analysed for their organic composition using Thermal Evolution, which was determined by using the Rock-Eval 6 Turbo at Geoscience Australia, Canberra. The raw samples were powdered in a puck mill and approximately 80 mg of sample was weighed into Rock-Eval crucibles. For pyrolysis the samples were kept at 300°C for 3 minutes then increased by 25°C/min. to a maximum of 650°C. For oxidation: 400°C for 4 min. then increased by 20°C/min. to 850°C.

#### *Organic-carbon-isotopes*

To determine how the  $\delta^{13}\text{C}_{\text{org}}$  record for Mossman fits into the global scheme, it was compared to the most complete and continuous carbon isotope record currently available for the Aptian. Menegatti et al. (1998) documented carbonate and organic carbon data for the uppermost Barremian-Aptian of the Italian Cismon section and the Swiss Roter Sattel section. Stratigraphic calibration relied on magnetostratigraphy, nannofossils and foraminifera; in accordance with Erba (1996) the base of the polarity Chron M0 was considered the base of the Aptian. These authors divided the record into eight C-segments (e.g., segments C1 to C8) based on characteristic changes in the  $\delta^{13}\text{C}_{\text{org}}$  curve, with the lower Aptian boundary in the middle of segment C2. Erba et al. (1999) published a more detailed (higher-resolution) carbon isotope record for the Upper Hauterivian-Lower Aptian of the Cismon section, in which particularly the nature of segment C2 appeared to be modified. To further determine the global extent of the segments, Bralower et al. (1999) selected a third area for organic-carbon-isotope study. They focused on Atlantic sections from northeastern Mexico and compared these to data from successions in the region. For easy correlation with the Tethyan Cismon section they adopted the terminology of Menegatti et al. (1998), and extended it upward with segments C9 to C15. In the present study we adhere to the recognition of the segments as defined by Menegatti et al. (1998) and Bralower et al. (1999), but for segment C2 the revised version of Erba et al. (1999) is applied.

Comparison of the organic-carbon-isotope record for Mossman and the Barremian-Aptian

records from Menegatti et al. (1998) and Bralower et al. (1999) shows similar stratigraphical variations (Figure 6). The top of segment C2 corresponds to an interval with progressively falling  $\delta^{13}\text{C}_{\text{org}}$  values, reaching a minimum in segment C3. In segment C4 the  $\delta^{13}\text{C}_{\text{org}}$  values show an abrupt increase, which is followed by an interval of relatively constant  $\delta^{13}\text{C}_{\text{org}}$  values characterizing segment C5. The black shales of the Selli Level fall within this segment (Menegatti et al., 1998). This interval is followed by further abrupt increase in  $\delta^{13}\text{C}_{\text{org}}$  values, characterizing C6. This leads to the extended Early Aptian organic-carbon-isotope maximum of segment C7. After C7 the  $\delta^{13}\text{C}_{\text{org}}$  values show an overall, long-term decrease, which corresponds to segment C8. At C9 the  $\delta^{13}\text{C}_{\text{org}}$  values show a sharp increase again. This is followed by  $\delta^{13}\text{C}_{\text{org}}$  values leveling out during C10. In the Mexican La Boca Canyon (Bralower et al., 1999; Figure 6) segment C11 shows a sharp decrease in the  $\delta^{13}\text{C}_{\text{org}}$  values to sharply increase again during segment C12.

## 4. Results

### 4.1 Palynology

In general, the samples contain relatively well-preserved palynomorphs; sporomorphs and dinocysts are abundant, acritarchs and acid-resistant foraminiferal linings are rare. Although sporomorphs dominate the assemblages in the investigated interval, dinocysts are well represented. The diversity of the dinocyst assemblages varies from relatively low to moderate (21 to 44 identified taxa; Table 3). Noteworthy is the amount of pyrite crystals observed in the interval from 74.16 - 93.28m.

#### *Palynostratigraphy*

The dinocyst assemblages have a cosmopolitan character. Stratigraphically important taxa occur in low numbers. The distribution of these key taxa is recorded in terms of first occurrence (FO) and last occurrence (LO) in time. Comparison of these FOs and LOs for Mossman to the ammonite calibrated dinocyst zonation schemes for the Tethyan and Boreal realms (Hoedemaeker and Leereveld, 1995; Wilpshaar, 1995; Leereveld, 1997; Hoedemaeker, 1999) as well as to sequences in Australia (e.g. Helby et al, 1987; Stover and Helby, 1987a, b; Helby and McMinn, 1992; Oosting et al., in prep.), reveals five important dinocyst events. In Mossman these age-diagnostic events in ascending order are (Figure 3):

1) FO *Tehamadinium sousensis* at 155.52m. In the Barremian type section at Angles (SE France) this event lies in the middle of the *sarasini* ammonite Chronozone of latest Barremian age (Oosting et al., in prep.). In the Boreal realm its FO lies in the *forbesi* ammonite Chronozone of earliest Aptian age (Lister & Batten, 1995; Heilmann Clausen & Thomsen, 1995).

2) FO of *Tehamadinium tenuiceras* is found at 127.26m. In the Tethyan realm, this event lies in the *tuarkyricus* ammonite Chronozone, according to Hoedemaeker and Rawson (2000) the lowest Aptian ammonite zone. In the Boreal realm it lies in the *deshayesi* ammonite Chronozone (Duxbury, 1983) in middle Lower Aptian.

3) FO of *Carpodinium granulatum* at 117.01m corresponds to the Boreal *germanica* belemnite Zone (compare with, e.g., Heilmann-Clausen and Thomson, 1995), and to the Boreal *pingue/innexum* ammonite Chronozone (Mutterlose, 1992; middle Upper Barremian).

4) FO of *Odontochitina operculata*. This event is found in sample 117.01m. In the Tethyan realm it lies in the lower *vandenheckii* ammonite Chronozone (Wilpshaar, 1995; lowermost Upper Barremian). In the Boreal realm its FO lies in the *elegans* ammonite Chronozone (Duxbury, 1980; lowermost Upper Barremian). This FO is considerably later in Australia than in Europe i.e., in the Aptian rather than in the middle Barremian (compare with Helby et al., 1987, figure 11).



Figure 3. (Facing page) The BMR Mossman-1 carbon isotope record, dinocyst events, and distribution in environmental dinocyst groups. Dinocyst events of global importance in bold font; of importance to the Helby et al. (1987) zonation scheme in normal font). C1-C12 corresponds to isotope segments; numbers 1-10 on right hand side correspond to dinocyst intervals.

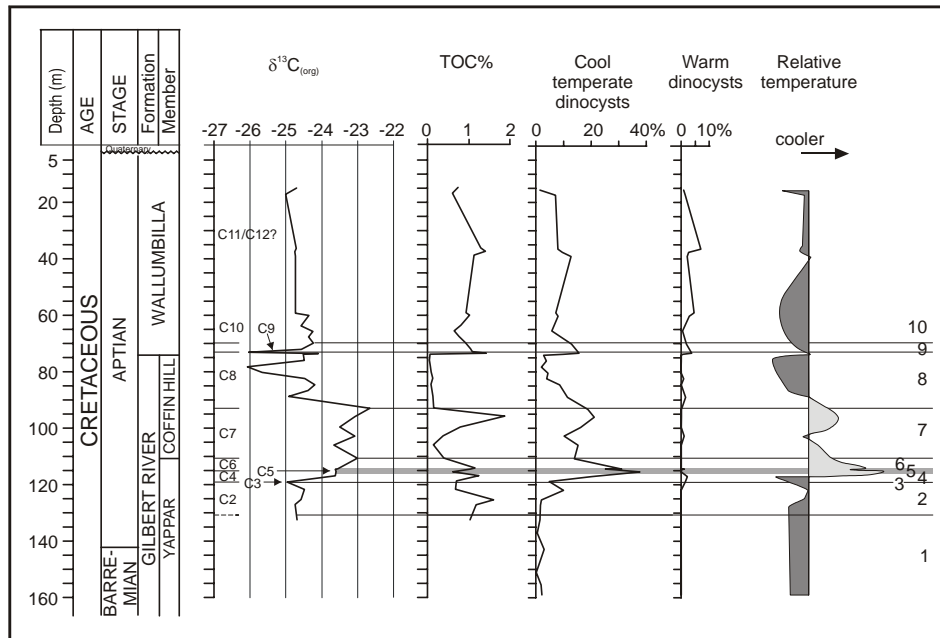


Figure 4. The BMR Mossman-1 carbon isotope record and TOC content combined with the cool/temperate and warm dinocyst groups, and relative temperature curve. C1-C12 corresponds to isotope segments; numbers 1-10 on right hand side correspond to dinocyst intervals.

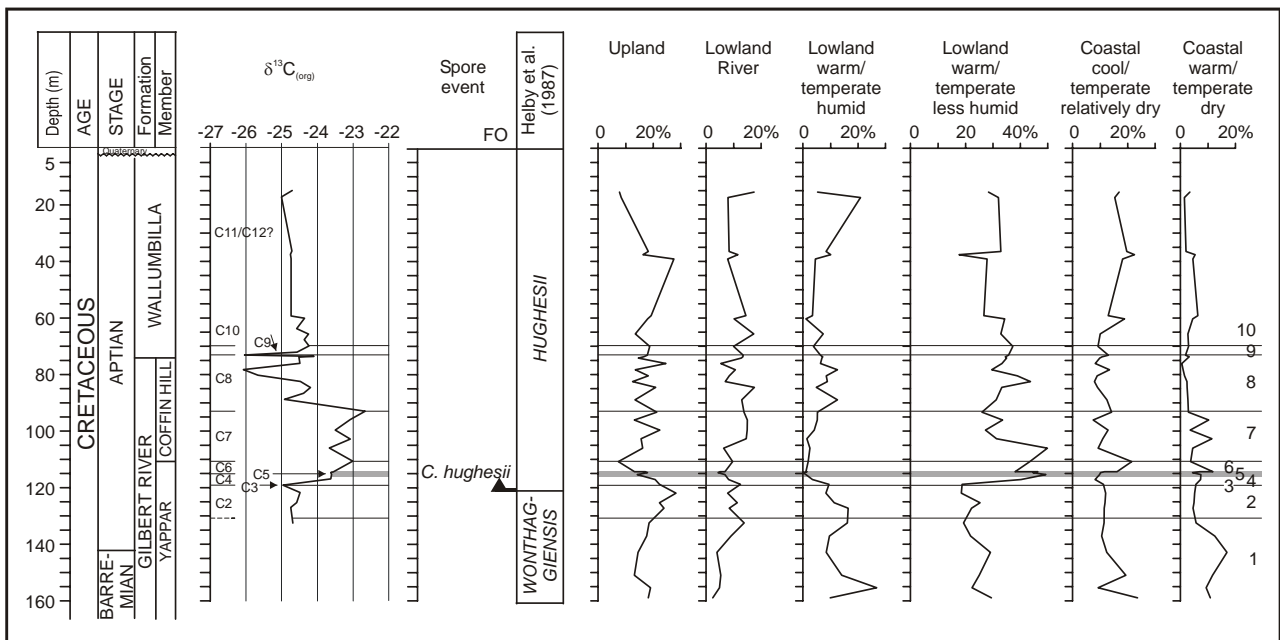


Figure 5. The BMR Mossman-1 carbon isotope record, event in spore/pollen groups of importance to the Helby et al. (1987) zonation scheme, and distribution patterns of environmental sporomorph groups (in percentage of total assemblage). C1-C12 corresponds to isotope segments; numbers 1-10 on right hand side correspond to sporomorph intervals.

5) LO of *Valensiella magna* lies in sample 110.88m. In the Tethyan realm it lies in the uppermost *sarasini* ammonite Chronozone (Oosting et al., in prep.). In NW Germany (Prössl, 1990) and in E England (H. Leereveld, unpublished) its LO is in an interval corresponding to the middle of the *O. germanica* belemnite Zone (middle Upper Barremian). Apparently this species reaches higher stratigraphic intervals in Australia than in Europe (compare with Helby et al., 1987, figure 26).

For stratigraphic correlation within the Australian region several other diagnostic events are recognized (Table 3; Figure 3): LO of *Canningia transitoria* (142.95m); FO of *Ovoidinium cinctum* (142.95m), its acme (121.96 – 137.06m), and LO (114.46m); LO of *Epitricysta vinckensis* (118.99m); FO of *Muderongia mcwhaei* (117.01m); LO *Muderongia australis* (106.22m); FO of *Diconodinium* spp (39.30m); FO of *Endoceratium polymorphum* (17.39m); coeval FO of *Spinidinium boydii* and *Diconodinium davidii* (15.32m).

Based on these first and last occurrences, the interval at Mossman comprises four of the Australian dinocyst zones defined by Helby et al. (1987). In ascending order these zones are: *Muderongia australis* Zone (from 159.05-142.95 m), *Ovoidinium cinctum* Zone (from 137.06-118.99 m), the *Odontochitina operculata* Zone (from 117.01-17.39 m) and, tentatively, the *Diconodinium davidii* Zone (at 15.32 m).

Images of key taxa are shown in Plate 5 and 6.

The main stratigraphically relevant FO datum within the spore/pollen assemblages is shown in Figure 5. The FO of *Cyclosporites hughesii*, which defines the boundary between the Austral *Foraminisporis wonthaggiensis* and *Cyclosporites hughesii* vegetation Zones (Helby et al., 1987), is recorded at 118.99 m.

#### *Palaeoenvironmental analysis*

The quantitative distribution patterns of the selection of palaeoenvironmentally significant dinocyst groups are depicted in Figure 3 and 4. General trends in the separate groups are discussed below.

The proxy for productivity, being the ratio of the heterotrophic to the generally autotrophic dinoflagellate types (Peridinioid-Gonyaulacoid ratio) shows remarkable strong fluctuations with distinct peaks at limited intervals. Taxa dominating the peaks are indicated.

The oceanic group is virtually absent, in particular in the lower and upper parts of the studied interval.

The outer neritic group is hardly present in the lower part of the studied interval, but forms the dominant constituent from 125.49 m upward.

The neritic group is mainly present in the lower and upper parts of the studied interval. Highest abundance of 17% is found at the base and frequencies gradually decline to zero at 110.88 m. From 76.26 m upwards frequencies, although severely fluctuating, gradually reach 10%.

The inner neritic group is the dominant constituent in the basal part of the studied interval (~50%) and rapidly declines towards 140 m core depth. Between 120 and 90 m the group is present with relatively higher frequencies to 12%. In the rest of the intervals representatives of this group were only occasionally recorded.

For the larger part of the studied interval frequencies of the littoral group fluctuate around 10%. Although, between 40-60 m it is virtually absent, and below 120 m it shows high abundances of up to 79%.

The low salinity group shows relative low and constant values in the lower part of the studied interval but values rapidly increase to 15% from 117.01 to 114.45 m. They then suddenly drop to 4% at 110.88 m. This is followed by a gradual increase again to 17% at 82.62 m, after which values gradually decrease towards the top.

The quantitative record of dinocyst types characteristic for cool/temperate climate zones is considered to reflect incursions of relatively cool waters in the Carpentaria Basin (Figure 4). These

dinocysts are virtually absent in the basal part, but with a sharp excursion at around 120 m they reach ultimate values (ca 38 %). Up to around 85 m values fluctuate and show a progressive decrease but remain between 10 to 20%, indicating the influence of relatively cooler waters. After the progressive decrease, the number in dinocysts associated with cool/temperate conditions culminates in an extreme low (ca 5%) between 85 and 75 m. Around 73 m values rapidly rise to 16%. This is shortly after followed by values fluctuating around 10% for the remainder of the studied section (70 m to top) indicating continued influence of cooler waters at the studied site.

The complementary dinocyst record reflecting warm influence (Figure 4) shows low values throughout the studied interval. In the basal part it is completely absent to show a minor peak around 118 m, just below the start of the strong increase in the cool/temperate group. Between 118 and 75 m the warm group is hardly present and only shows minor peaks at four separate levels. Above 75 m the group is consistently present and fluctuates around 5%. This group combined with the cool/temperate group was used to infer the relative temperature variations in Mossman (Figure 4).

The quantitative distribution patterns of the palaeoenvironmental sporomorph groups are depicted in Figure 5 and given in Table 4. General trends in the separate groups are discussed below.

The lowland - warm/temperate and less humid - group largely dominates the sporomorph associations throughout the studied interval (fluctuating between 17% and 50%) with consistently high values in the middle part.

The upland group (shifting around 20%) and coastal, cool/temperate and dry group (fluctuating between 7% and 22%) are both well represented throughout the studied interval.

With exception for the lower part of the studied interval where the lowland/river group reaches relatively low numbers, its frequency shifts around 10%.

In the curve of the lowland, warm/temperate and humid group three parts can be distinguished. In the lower part a decrease from over 20% (at 155.52 m) to zero (at 114.69 m) is apparent. Upward in the middle part, frequencies gradually reach maximum values around 12% and decline again to near absence. In the upper part higher values gradually regain (to just over 20%).

Apart from the basal part of the studied interval where an abundance of 17% is recorded the coastal warm and dry group is only present in low frequencies (occasionally reaching 10%).

## 4.2 Geochemistry

Given the fine-stratigraphic assessments from dinocyst correlation in this study, the  $\delta^{13}\text{C}_{\text{org}}$  curve for Mossman compares well with global Barremian-Aptian records from Menegatti et al. (1998), Bralower et al. (1999) and Erba et al. (1999). The lowest segment C1 and highest segments C13-15 are not represented in the set of chemostratigraphic samples from Mossman. For the rest remarkable similar stratigraphic variations are apparent (Figure 6). The chemostratigraphical data for Mossman-1 is given in Table 5.

The basal Aptian interval with relatively high  $\delta^{13}\text{C}_{\text{org}}$  values of segment C2 is recognized in Mossman between 132.52-118.99 m. In the global carbon curve segment C2 is normally followed by the sharp negative excursion of segment C3 (Menegatti et al., 1998; Bralower et al., 1999). The Mossman data do not document this strong negative excursion, but do show the successive, abrupt increase in values associated with C4. The global  $\delta^{13}\text{C}_{\text{org}}$  segment C3 has therefore tentatively been put at the lowest value for Mossman, at 118.99 m (-25‰); segment C4 is identified from 118.99-115.47 m. This is followed by an interval of relatively constant  $\delta^{13}\text{C}_{\text{org}}$  values indicative of C5 (115.47-114.45 m). Successively the  $\delta^{13}\text{C}_{\text{org}}$  values strongly increase, characterizing segment C6 (114.45-110.88 m). This in turn precedes an interval inferred to represent the extended Early Aptian carbon isotope maximum of segment C7 (110.88-93.28 m). After C7 the  $\delta^{13}\text{C}_{\text{org}}$  values show an overall, long-term decrease, which corresponds to the nature of segment C8 (93.28-73.27

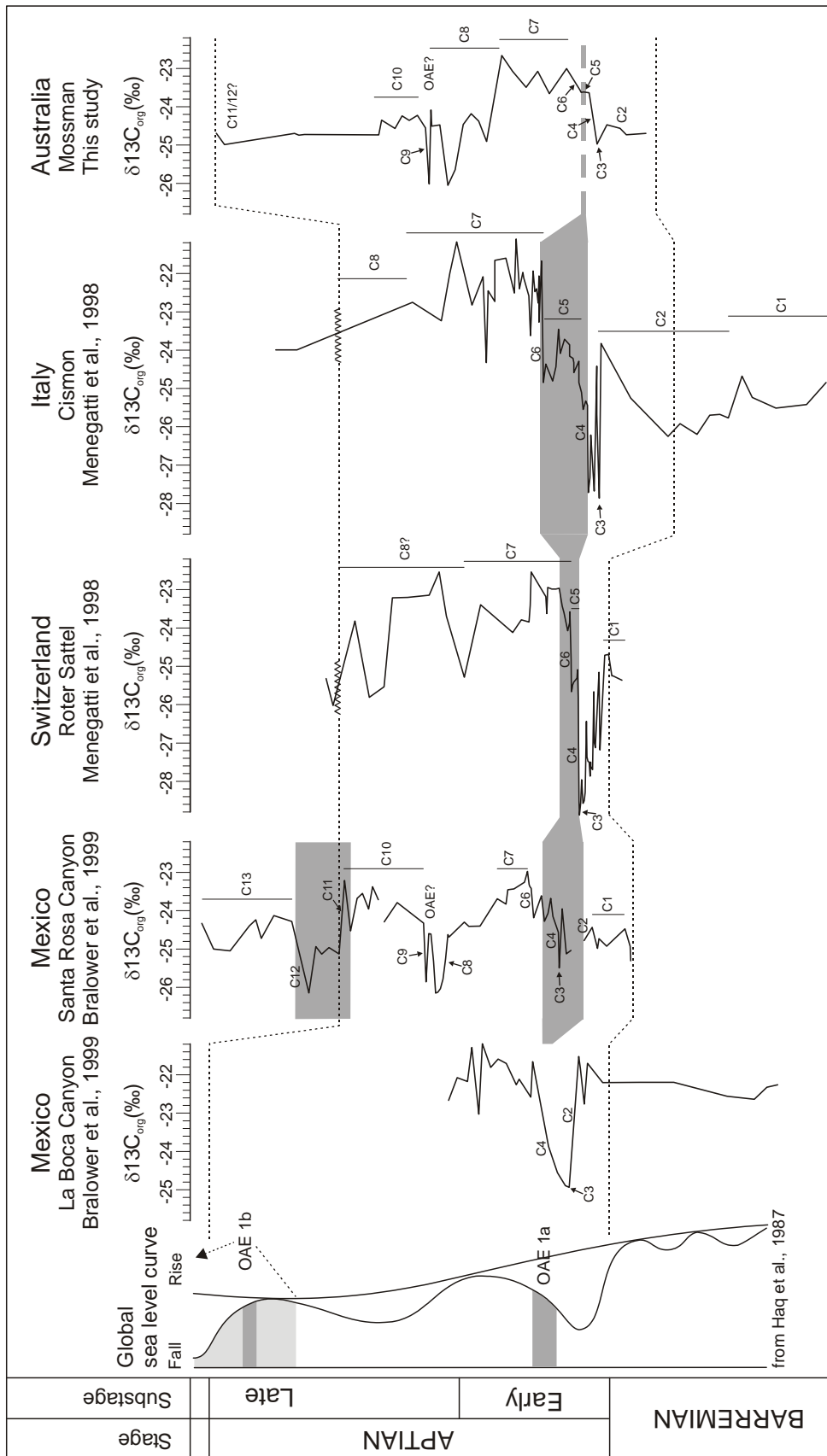


Figure 6. Correlation of  $\delta^{13}C_{org}$  records from BMR Mossman-1, Australia (this study), La Boca Canyon and Santa Rosa Canyon sections from Mexico (Bralower et al., 1999), and the Roter Sattel (Swiss) and Cison (Italy) sections (Menegatti et al., 1998). Labels C1 to C13 represent segments of the  $\delta^{13}C_{org}$  curves and are discussed in the text.m).

The following interval shows sharply increasing  $\delta^{13}\text{C}_{\text{org}}$  values again characterizing segment C9 (73.27-70.11 m). This segment is succeeded by an interval with relatively constant values, corresponding with segment C10. Unfortunately, core between 18.29-36.57 m and 39.62-59.44 m was not recovered and a solid comparison with younger segments cannot be established but it probably contains segments C11 and C12, although their characteristics are not discernable.

#### *Total organic carbon content*

Deposition at Mossman occurred in a marginal to open marine setting but conditions seem to have been such that part of the TOC was preserved for most of the studied interval (Figure 4). Although, most of the samples analyzed contain less than 1% TOC (Table 5), five peaks with up to 1.9% TOC are observed: two in the Yappar Member, one in the Coffin Hill Member, and two in the Wallumbilla Formation. These peaks in TOC content in general correlate with maxima in the cool/temperate dinocyst group (Figure 4).

The lowest TOC has been measured for the upper half of the Coffin Hill Member (from 74.16 to 93.28 m) with values not exceeding 0.1%, corresponding to the interval with the lowest values in gamma ray (Figure 2) and the highest amount of pyritised palynomorphs observed for this study. The extreme low TOC-values may also be due to extensive bioturbation in this particular interval as noted by Smart and Grimes (1971).

#### *Rock-Eval*

A sample for each of the five peaks shown in the TOC record was used for Rock-Eval analysis. However, four of the five samples have hydrogen index (HI) and oxygen index (OI) values that plot close to the origin, revealing little about source or thermal history (Table 6).

## **5. Integration and interpretation of results**

In this section firstly the biostratigraphic assessment will be highlighted in order to put the inferred palaeoenvironmental changes at Mossman into a global perspective. Secondly, by means of an integrated approach the many variables (sporomorphs and dinocyst palaeoenvironmental groups, geochemical data, lithology) are interpreted towards a coherent development of the local palaeoenvironmental changes at Mossman. Thirdly, an attempt is made to discriminate between the nature of the local and the global (climatic) changes, with emphasis on 2<sup>nd</sup> and 3<sup>rd</sup> order eustatic sea-level fluctuations (sequence stratigraphic signature) and global organic-carbon-isotope record.

### *5.1 Biostratigraphic assessment*

#### *Dinostratigraphy*

Based on the successive FOs of *T. sousensis*, at 155.52m, and *T. tenuiceras*, at 127.27 m (Figure 3), the lower part of the studied interval at Mossman directly correlates to uppermost Barremian. *T. sousensis* is documented from the *sarasini* ammonite Chronozone of uppermost Barremian and *T. tenuiceras* from the *tuarkyricus* ammonite Chronozone of lowermost Aptian (Erba, 1996). The Barremian-Aptian boundary is tentatively put between these two FOs at ~145 m (see later for a detailed assessment based on integrated chemostratigraphy, biostratigraphy and sequence stratigraphy). In Europe the inception of *T. sousensis* is associated with the LO of *V. magna* (Oosting et al., in prep.), seemingly different from Australia where this taxon is reported to range into the Lower Aptian (compare e.g. Helby et al., 1987), which is also the case in Mossman (LO of *V. magna* at 127.27 m).

Another taxon showing deviating stratigraphic ranges in Australia and Europe is *C. granulatum*. It incepts extremely high in Mossman (at 117.01 m), in the Lower Aptian, instead of showing an uppermost Barremian FO as in northwestern Europe (Heilmann-Clausen and Thomson, 1995). This is probably due to specific environmental circumstances, which only later became favorable for *C. granulatum* at Mossman (e.g., cooler/temperate climatic conditions).

For pan-Australian correlation the first high frequency of *O. cinctum* at 137.06 m in Mossman marks the base of the *O. cinctum* Zone and, consequently, the top of the stratigraphically older *M. australis* Zone. The zonal boundary between these zones is accordingly placed between samples 137.06 and 142.95 m (Figure 3). In support of this, the LO of *Canningia transitoria*, reported by Stover and Helby (1987b) from a similar position in the *M. australis* Zone from the Houtman-1 well, lies at 142.95 m.

The top of the strongly facies-controlled *O. cinctum* Zone is defined by the marked decrease of *O. cinctum* (Helby et al., 1987). This event is normally coeval with the first consistent occurrence of *O. operculata* which defines the base of the succeeding *O. operculata* Zone. In Mossman the *O. cinctum* Zone is well developed with the acme from 121.96-137.06 m. The boundary between the *O. cinctum* and *O. operculata* zones is therefore put at the level of marked decrease of *O. cinctum*, between samples at 118.99 and 121.96 m. Placement of the zonal boundary is further supported by the LOs of *E. vinckensis* and *M. australis* which are just above this level, in the lower *O. operculata* Zone (Helby et al., 1987).

The strong facies dependence of the *O. cinctum* Zone makes that it is not consistently developed throughout Australia (Helby et al., 1987). In case the zone is absent, the FO of *M. mcwhaei* is alternatively used to define the base of the *O. operculata* Zone (Helby, 1987; Helby et al., 1987).

In Mossman the coeval FOs of *Odontochitina operculata* and *M. mcwhaei* at 117.01 m (Figure 3) is remarkable in that the first taxon usually incepts at slightly lower stratigraphic levels in Australian sequences than *M. mcwhaei* (compare e.g. Helby and McMinn, 1992; Oosting et al., in prep.). It should be noted that *O. operculata* shows a considerable later FO in Australia than in Europe, in the Aptian rather than in the middle Barremian.

The first appearances of *Diconodinium* spp and *S. boydii* (at 15.32 m) are indicative of the Australian upper *O. operculata* Zone. The acme in *D. davidii* is characteristic for the next higher *D. davidii* Zone. Although the FO of *Endoceratium turneri* (marking the base of the *D. davidii* Zone) was not observed, the morphologically close *E. polymorphum* does appear at 17.39 m. Consequently the top of the studied interval at Mossman is tentatively assigned to the *D. davidii* Zone (at 15.32m). In accordance with this, the preceding *O. operculata* Zone ranges between 118.99 and 17.39 m (Figure 3).

Because Late Aptian or Albian markers were not encountered, the studied interval (159.05 to 15.35 m) is inferred to represent latest Barremian and Early Aptian deposits, probably Late Aptian in the upper part.

#### *Sporomorph stratigraphy*

Two of the eastern Australian sporomorph zones (Helby et al., 1987) are identified at Mossman: the *Foraminisporis wonthaggiensis* and *Cyclosporites hughesii* zones. The boundary between these zones is put at the FO of *C. hughesii* (121.96m; Figure 5). The succeeding *Crybelosporites striatus* Zone with an inferred Albian age (Helby et al., 1987) was not recognized. This supports the assumption that the deposits from Mossman are not younger than Aptian.

## 5.2 Reconstruction of local palaeoenvironmental changes

### *Interpretation of dinocyst record*

Following the successive abundance peaks in the curves of the selected palaeoenvironmental dinocyst groups (Figure 3 and 4), the basal part of the studied Mossman section (uppermost Barremian to Aptian boundary interval) is interpreted to represent neritic relatively warm temperate conditions. Here, low salinity waters had virtually no influx and outer neritic influence was absent. Just prior to the Aptian (~145 m core depth) a profound temporary drop of sea level to more inner neritic conditions is apparent.

Successively, the 137.06 m level represents a drastic sea-level drop to littoral conditions, associated with a rapid increase in the heterotrophic *O. cinctum*, a littoral element. This species dominates dinocyst assemblages until 121.96 m, while typical cool temperate dinocysts are still hardly present. The interval characterized by the *O. cinctum* acme (121.96-137.06 m) is succeeded by an interval reflecting a distinct sea-level rise from littoral to outer neritic conditions at Mossman, which from then on prevail in the investigated interval. This rapid transgression is accompanied by the first, but extremely limited influence of oligotrophic waters and by a major influx of cool temperate waters. The following relative high in sea level is reflected by the main outer neritic influence with occasional oceanic elements but undergoing clear neritic input as well. After a severe drop of inner neritic influx to virtual absence (89.04 m), outer neritic, relatively cool water conditions progressively decrease, and in reverse, low salinity and littoral influx gradually increase. During this apparent fall of sea level, low-salinity influx reaches its peak value (associated with a relatively restricted abundance of the heterotrophic element *A. acribes* (at 74.16-89.04 m). After the fall in sea level outer neritic conditions are rapidly restored (from 73.90 m) coeval with returning cool temperate influence. Towards the top of the investigated interval falling sea level is reflected by increasing influx of elements derived from shallower parts on the shelf (neritic to littoral), with a distinct peak in the heterotrophic *D. davidii* at the top.

### *Interpretation of sporomorph record*

A reconstruction of the progressive vegetation development on the land adjacent to the Mossman site is depicted in Figure 7. Going upward in the studied interval, the quantitative distribution patterns of the selected palaeoenvironmental sporomorph groups (Figure 5) show the most prominent long-term changes in the development of the dry lowland vegetation and the warm temperate coastal vegetation. In the first group a shift is apparent to consistently higher representation (at 117.01 m), largely at the cost of the humid lowland vegetation, which gradually diminishes to near absence.

The extension of the cool temperate coastal vegetation seems to change only slightly without real apparent tendencies. The same holds for the upland vegetation. River influence is constantly present, but to a minor extent only in the basal part of the studied interval.

A more detailed reconstruction of the successive developments of the terrestrial environment will be dealt with in the next paragraph.

### *Integration of results based on organic-carbon-isotope segments*

The latest Barremian-Early Aptian (?Late Aptian) age assessment for the studied interval here enables comparison of the  $\delta^{13}\text{C}_{\text{org}}$  record for Mossman and global organic-carbon-isotope records. Correlation reveals close similarity, and in the sequence of events in the  $\delta^{13}\text{C}_{\text{org}}$  record from Mossman the global isotope segments as defined by Menegatti et al. (1998) and Bralower et al. (1999) can be identified; see segments C2-10 in Figure 6. The segments recognized are considered steps in the latest Barremian-Aptian environmental development at Mossman, in perspective of global environmental change. The distinguished steps are discussed here in ascending order, with the biostratigraphic assessments derived from the present study. In the basal and top parts of the studied section segments could not be identified, because (1) for the basal part

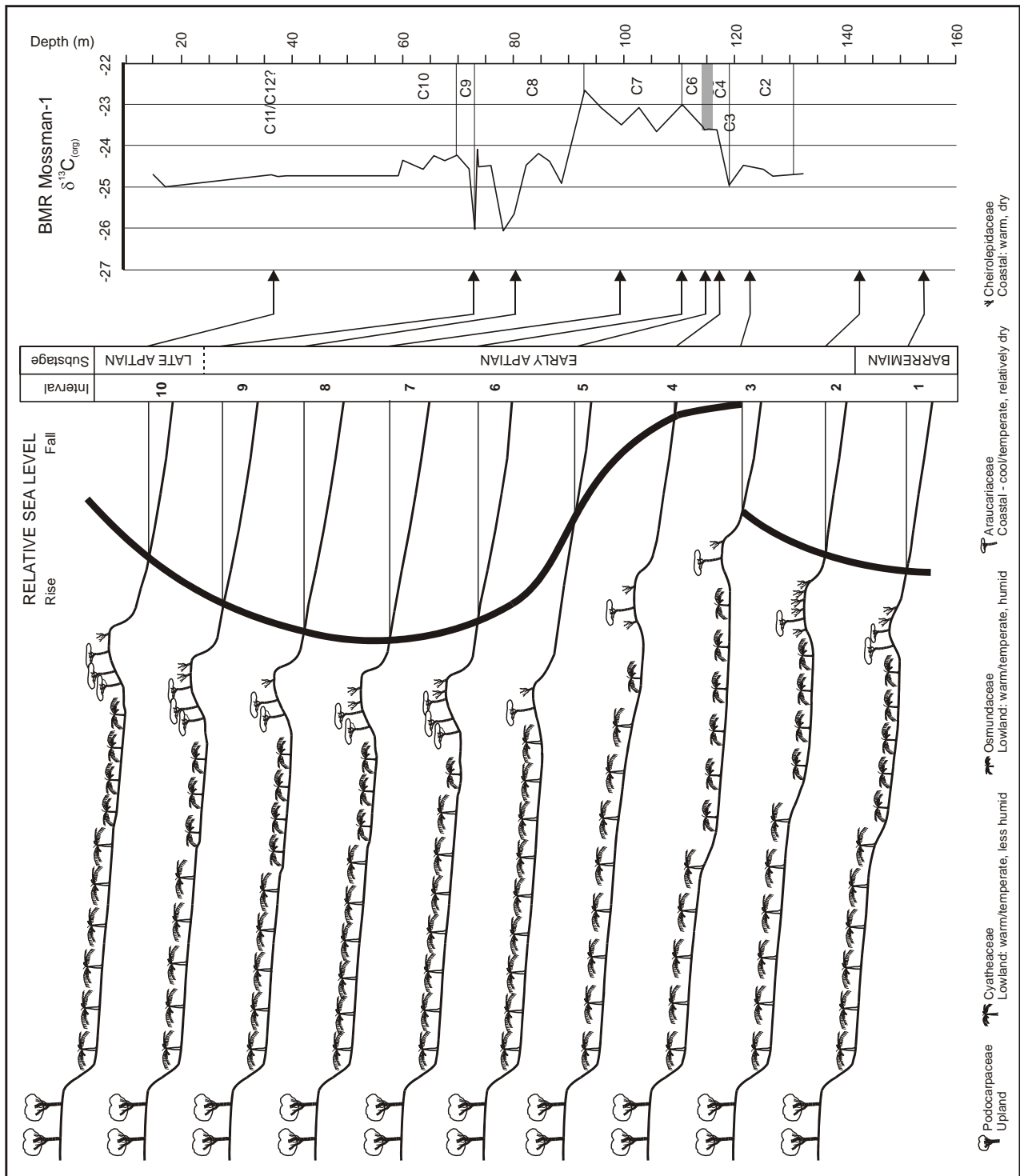


Figure 7. Palaeoenvironmental and sea-level reconstructions for BMR Mossman-1, based on distribution within the spore/pollen groups; numbers 1-10 correspond to sporomorph intervals. Arrows indicate the approximate level to which the reconstruction correlate in the carbon isotope curve.

chemostratigraphic data are not available, and (2) for the top part resolution is too low.  
**Basal interval (1):** 132.52-159.05 m (uppermost Barremian - lowermost Aptian). Dinocysts indicate a progressive palaeoenvironmental shift from neritic to littoral, associated with a rapid increase in productivity. The extended period of high productivity corresponds with a lithologic interval containing several pebbly beds; at 155.5-155.8 m a pebbly conglomerate, and at 139.4-143.7 m pebbly beds are present. The terrestrial record does not seem to reflect progressive

changes accordingly, although the most extensive development of warm and dry coastal circumstances are documented from this interval. The decline of the warm and dry coastal group towards the top of the interval seems to occur in favor of extension of a river dominated landscape (which, however, is not reflected in enhanced fresh water influx in the basin). The interval represents the period of progressively increasing fall of sea level and successive prolonged sea-level lowstand.

**Segment C2:** 121.96-132.52 m (lowermost Aptian). Littoral palaeoenvironments prevail over most of the interval while towards the top the inner and outer neritic influence increases, accompanied by a slight cooling effect and a sharp drop in productivity. In the terrestrial record the upland vegetation progressively migrates basinward, seemingly at the cost of humid conditions in the adjacent lowlands. Apart from the upper part of the segment, TOC values are relatively high. The lithologic unit consisting of coarse quartz sands (from 123.7-125.2 m) and referred to as 'Artesian flow' (Figure 2; Grimes and Smart, 1971) is here considered to reflect a major drop in sea level. The segment overall thus represents rapid but progressively decreasing fall of sea level. Possibly it is accompanied by hiatuses within the sandstone deposits, which probably obscure the extreme negative  $\delta^{13}\text{C}_{\text{org}}$  values (characteristic for the Aptian boundary: compare with Erba et al., 1999) in Mossman.

**Segment C3:** 118.99 m (lowermost Aptian). This level marks a distinct change in the palaeoenvironment on land and in the sea at the Mossman site. The warm temperate/humid lowland vegetation is strongly reduced while the warm temperate/drier vegetation expands. Likewise, below (and including) this level, littoral palaeoenvironments prevail contrary to the interval above, where outer neritic conditions seem to persist. A temporary relative rise in sea temperature is noticeable. This level is interpreted to represent the beginning of a distinct sea-level rise.

**Segment C4:** 117.01-118.99 m (lowermost Aptian). The dinocyst palaeoenvironmental distribution patterns indicate a remarkable single incursion of oceanic waters (coinciding with low productivity conditions), together with increased influence of relatively cool outer neritic waters, but with extremely limited littoral influx. On land a profound shift in the lowland vegetation from humid to drier circumstances, together with strong withdrawal of the upland vegetation, is apparent. The segment represents the period of fastest rise of sea level.

**Segment C5:** 114.45-117.01 m (lowermost Aptian). The short interval is characterized by marine conditions at Mossman in the joint prevalence of outer neritic and cool temperate waters. At its top low-salinity influx reaches a maximum, and a single peak in heterotrophic elements (*Palaeoperidinium cretaceum*) indicates regained bottom transport from shallower areas on the shelf. The upper half of the segment consists of the only distinct shale bed reported from the studied interval at Mossman (Smart and Grimes, 1971; Figure 2). In the terrestrial record, this segment shows the maximum extension of the warm temperate/relatively dry lowland vegetation reached, whereas its warm temperate/humid counterpart has virtually disappeared. The segment reflects the first signs of slackening just after the most rapid phase in sea-level rise.

**Segment C6:** 110.88-114.45 m (Lower Aptian). In the interval, neritic and outer neritic conditions change to inner neritic with littoral influence. This coincides with a slight warming of seawater temperatures, indicated by the minor decrease in the cool/temperate dinocyst group. This segment represents a continued slackening transgression. On land the coastal zone restores, mainly on account of the lowland and upland vegetation area.

**Segment C7:** 96.09-110.88 m (Lower Aptian). Within this interval relatively cool outer neritic conditions prevail, but with a clear inner neritic and littoral contribution. Progressive increase of river input coincides with a consistently expanding fresh-water vegetation cover on the lowland. Upland vegetation gradually approaches again and, in reverse, the warm temperate/less humid lowland vegetation distinctly declines. The base of the segment approximates the base of the Coffin Hill Member. Going upward in the segment the TOC values rise drastically to reach the

highest value within the studied interval of de Mossman section. The segment represents the period of continuing rise in sea level towards its maximum flooding at the top.

**Segment C8:** 73.90-96.09 m (Lower/?Upper Aptian). The top of this interval corresponds to a major change in lithology, being the boundary between the typical coarse-clastic Gilbert River Formation and the more open-marine Wallumbilla Formation. Within this interval outer neritic and relatively cool conditions coevally declined in favor of relatively warmer shallower neritic waters. Low salinity influx reached ultimate values and was accompanied by two pulses of enhanced local productivity (the higher one is associated with increased littoral influx); in contrast, inner neritic influence nearly disappeared. On land warm temperate/dry coastal vegetation was severely reduced and the warm temperate/humid lowland vegetation covered the area; no further distinct changes are apparent. Throughout the entire interval TOC values are extremely low, and pyrite content extremely high, probably due to (anoxic) bacterial activity consuming organic matter. The segment represents a period of progressively falling sea level towards prolonged low levels followed by a short rise.

**Segment C9:** 70.11-73.90 m (lower/?upper Aptian). In this interval outer neritic conditions with cool temperate influence are restored again with contribution (although relatively small) of neritic and low salinity elements. No real changes in vegetation on the adjacent land took place. Most noteworthy about this interval is a raised TOC content. The segment represents the period of rapidly rising sea level.

**Top interval (10):** 15.32-70.11 m (?upper Aptian). Although no drastic changes are apparent in the outer neritic relatively cool temperate marine palaeoenvironment, it must be realized that sample resolution in this interval is beyond detecting changes at the scale as before. The overall trend of the low salinity influx is a progressive decline in contrast to the (inner) neritic and littoral contribution. On land the coastal system with vegetation tolerating cooler climate and the lowland warm temperate/less humid vegetation cover gradually expand seaward enlarging the distance between the site of deposition and the upland vegetation. The top of this interval is marked by an acme of the dinocyst *D. davidii* and a change in lithology, from mudstone with minor sandstone to pebbly, sublittoral sandstone with minor shale and mudstone.

The basal part of interval 10 represents the end of a short-term transgression. This is succeeded by a long-term cycle with diminishing rise of sea-level, its successive maximum transgression and subsequent sea-level fall toward the top of interval 10.

### 5.3 Sequence stratigraphy

The local sea-level fluctuations deduced at Mossman are considered to reflect the (global) 2<sup>nd</sup> and 3<sup>rd</sup> order sequence stratigraphic signature (Hardenbol et al., 1998; Jacquin et al., 1998). The apparent fluctuations and contemporaneous vegetation development are depicted in Figure 7 and 8. The basal part of the studied section is interpreted to reflect the 2<sup>nd</sup> order Regressive Subcycle R12d of Jacquin et al. (1998) (Figure 8), comprising a series of Highstand Systems Tracts of uppermost Barremian-lowermost Aptian 3<sup>rd</sup> order cycles Ba6, Ap1 and Ap2. Lithologically the respective sequence boundaries are recognized at the base of the pebble conglomerate at 155.5-155.8 m (Ba6: 121.8 My), the pebbly beds at 139.4 - 143.7m (Ap1: 121.0 My) and 'Artesian flow' at 127.6-131.5 m (Ap2: 120.6 My). In Hardenbol et al. (1998), and Jacquin et al. (1998), Ap1 defines the stage boundary. This puts the base of the Aptian for the studied section from Mossman at 143.7 m (in between the FOs of *T. sousensis* and *T. tenuiceras*; Figure 3 and 8).

The entire regressive interval comprising the upper part of Subcycle R12d of Jacquin et al. (1998) is palynologically characterized by the dominance of the dinocyst *O. cinctum*. This supports the view advocated by Helby et al. (1987) and Loutit et al. (1997) that the *O. cinctum* Zone is associated with shallow marine environments and extensive river systems. These authors used this

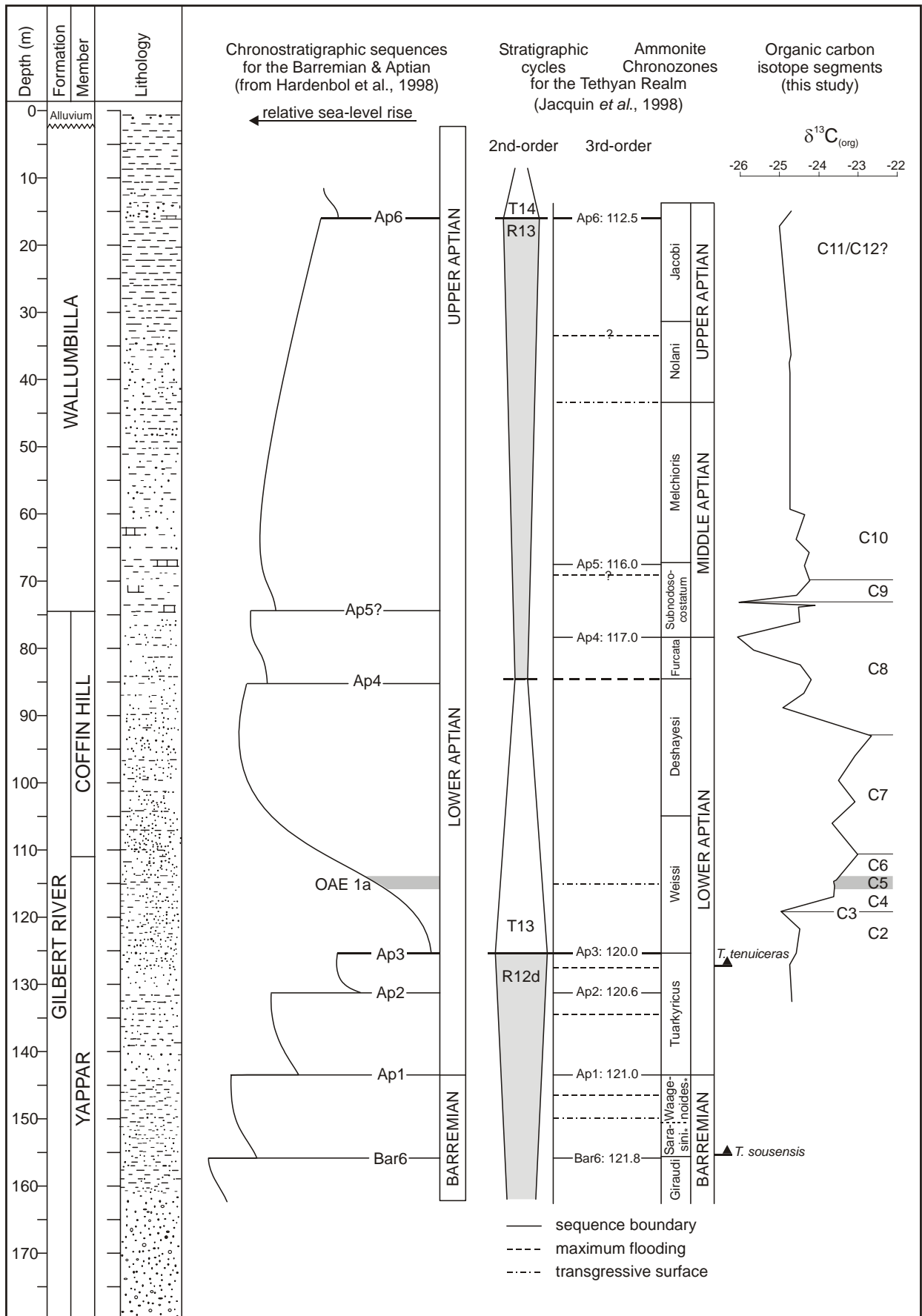


Figure 8. Correlation for BMR Mossman-1 of: lithology, sea-level reconstructions (based on Hardenbol et al., 1998; and Jacquin et al., 1998), and isotope signature. Zones marked with an '\*' are the latest Tethyan ammonite Chronozones (Hoedemaeker and Rawson, 2000). Dinocyst events are taken from this study.

strong environmental dependence to explain why the *O. cinctum* Zone is not consistently found in Australian sections.

Immediately above the inferred Ap2 sequence boundary the dinoflagellate *T. tenuiceras* first occurs, implying its position in the *tuarkyricus* ammonite Zone. Successively, the next higher interval with pebbles (at 123.7-125.2 m), marking profound palaeoenvironmental changes, is inferred to reflect major sequence boundary Ap3 of Jacquin et al. (1998). At Ap3 *O. cinctum* still dominates the dinocyst assemblages but shows a sharp decrease immediately above this level (at 118.99 m). If Ap3 indeed marks the base of the *weissi* ammonite Chronozone (Jacquin et al., 1998; Figure 8) the Australian *O. cinctum* Zone consequently correlates to the European *tuarkyricus* and lower *weissi* ammonite zones.

Sequence boundary Ap3 further forms the start of the 2<sup>nd</sup> order Transgressive Phase T13 (Jacquin et al., 1998) culminating at peak transgression (at 96.09 m in Mossman, the boundary between global organic-carbon-isotope segments C7 and C8). The boundary between the Yappar Member and Coffin Hill Member is situated in the Transgressive Systems Tract of the Ap3 cycle.

The following Regressive Phase R13 of Jacquin et al. (1998), including the two 3<sup>rd</sup> order cycles Ap4 and Ap5, is possibly contained in the upper part of the studied interval of the Mossman section. Ap4 (117.0 My) is recognized in the upper part of the Coffin Hill Member, approximately at 78.38m. The palynological assemblages just below this level show a decrease in all but the littoral dinocyst groups, reflecting a short-term relative fall in sea level. The boundary between the Gilbert River Formation and Wallumbilla Formation marks a lithologic change from glauconitic sandstones to mudstones (Figure 2) and is inferred to reflect the Transgressive Surface of the Ap4 cycle. Sample density in the upper part of the studied interval is too low to enable a reliable approximation of the sequence boundary Ap5 (116.0 My) based on dinocysts. Lithologically the level at 67.80m with the transition from mud and limestone to an interval with mainly glauconitic sandstone forms a good candidate.

The extreme dominance of the heterotrophic dinocyst *Diconodinium davidii* in the pebbly sandstone interval amidst mudstones in the top of the section (between 13.7-15.8 m) indicates a sea-level drop. It is inferred to represent sequence boundary Ap6 (112.5 My) of Jacquin et al. (1998), which approximates the Albian boundary (Figure 8).

## 6. Discussion

Biostratigraphic correlation of dinoflagellate cyst events shows that the studied interval from the BMR Mossman-1 well corresponds to uppermost Barremian and Aptian. A detailed biostratigraphy of the top is missing but it probably corresponds to Upper Aptian since biomarkers for the Albian are absent. Direct correlation of an Australian sequence with Barremian-Aptian ammonite calibrated Tethyan and Boreal successions revealed nine possible dinocyst events useful for global biostratigraphic correlation (Oosting et al., in prep.). Of these, five were recognized in the investigated interval from Mossman: the FO of *T. sousensis*, FO of *T. tenuiceras*, FO of *C. granulatum*, FO of *O. operculata*, and LO of *V. magna* (Figure 3). Although the order of events at Mossman differs from the calibrated events, they can be used to approximate the Aptian stage boundary.

In the Barremian type section at Angles (Birkelund et al., 1984) the dinocyst species *T. tenuiceras* first occurs just above (ca 1m) the traditional Aptian boundary (Oosting et al., in prep.) i.e., in basal *tuarkyricus* ammonite Zone (Delanoy et al., 1997). Based on carbon isotope correlation Wissler et al. (2002) substantiated that the internationally recommended Barremian-Aptian boundary (i.e., the base of magnetic polarity Chron M0: Erba, 1996) is situated about 2m lower in Angles (in the “non characterized zone” of Delanoy, 1997). In Mossman *T. tenuiceras* appears in between sequence boundaries Ap2 and Ap3 (R12d in Jacquin et al., 1998; Figure 8), corresponding to a level within the *tuarkyricus* ammonite Chronozone.

In Mossman, regressive subcycle R12d (Jacquin et al., 1998) is most strongly reflected by heterotrophic dinocysts dominating the palynomorph assemblages. In this particular interval *O. cinctum* forms the most abundant constituent, on which basis the Australian *O. cinctum* dinocyst Zone of Helby et al. (1987) is identified. From a palaeoenvironmental point of view its presence supports the inferred strongly facies dependant nature as advanced by Helby et al. (1987) and Loutit et al. (1997). The overall neritic character of the dinocyst assemblages in Mossman and its presence associated with a 2<sup>nd</sup> order sea-level drop confirms the restricted marine association of the acme zone (compare with Loutit et al., 1997). In accordance with this, the zone may poorly show or be absent in deeper marine settings, e.g. as in ODP 763 (Brenner, 1992) and DSDP site 263 (Oosting et al., in prep.).

Helby et al. (1987) suggested the Barremian-Aptian boundary to fall within the *Ovoidinium cinctum* Zone. This implies that the acme zone would correlate to the standard uppermost Barremian *waagenoides* and basal Aptian *tuarkyricus* ammonite Chronozones. Based on direct biostratigraphic correlation with ammonite-controlled sections however, the present study shows that the acme zone is slightly younger and correlates with the Aptian *tuarkyricus* and lower *weissi* ammonite Chronozones. The Barremian-Aptian boundary consequently falls within the top of the preceding *M. australis* Zone. Because of the inferred Aptian age for the remainder of the studied section at Mossman, the entire *O. cinctum* Zone, the successive *O. operculata* Zone, and the lowermost *D. davidii* Zone are Aptian. Based on the calibrated levels in Australia the boundary of the *F. wonthaggiensis* and the succeeding *C. hughesii* sporomorph zones, originally inferred to fall within the Lower Aptian (Helby et al., 1987), is slightly younger than initially inferred.

The biostratigraphic correlation developed from this study has refined age assignment for lithostratigraphic units intersected in Mossman-1. The Yappar Member is of latest Barremian-earliest Aptian age instead of undifferentiated Neocomian, as indicated in previous assessments (summarized in Morgan, 1980). At Mossman the entire Coffin Hill Member is assigned to the Aptian and does not comprise Neocomian as well, as inferred previously (see Morgan, 1980). The interval represented by the Wallumbilla Formation in Mossman is also exclusively Aptian in age.

To detect how the local conditions during the latest Barremian-Aptian at Mossman were affected by eustatic sea-level variations, the quantitative palynological data from this study were put in a sequence stratigraphic perspective (charts of Hardenbol et al., 1998 and Jacquin et al., 1998). It appeared that all 2<sup>nd</sup> order transgression-regression fluctuations were detected and that all 3<sup>rd</sup> order variations could be identified (cycles Ba6 and Ap1 to Ap5; Figure 8).

Morgan (1980b) recognized that the Early and Middle Cretaceous sedimentary architecture in the Australian basins resulted from global sea-level fluctuations. For the Carpentaria Basin he proposed five transgressive phases of latest Barremian-Aptian age (Morgan, 1980b, figure 22). In his view the presumed fluvatile Yappar Member represents the first transgressive phase and the boundary with the overlying marginal to open marine Coffin Hill Member reflects end transgression. In accordance with Burger (1982, figures 2 and 12), the present study supports a shallow marine depositional palaeoenvironment for the upper part of the Yappar Member, rather than exclusively being of fluvatile origin (e.g. Morgan, 1980b). The next lithologic unit, the Coffin Hill Member, represents the second transgressive phase in Morgan (1980b), and the boundary with the following Wallumbilla Formation as end of the phase. In the strong Aptian transgression represented by the open marine lower Wallumbilla Formation he recognized two separate phases in sea-level rise, although their separation is not reflected by a lithologic boundary. The youngest transgressional phase is indicated to end deeply and abruptly near the Albian boundary (Morgan, 1980b). Slightly deviating from his interpretation, the present study shows that the lithologic boundaries (Gilbert River Formation-Wallumbilla Formation and Yappar Member-Coffin Hill Member) represent progressive steps to more open marine facies. These boundaries are here inferred to fall in Transgressive Systems Tracts of cycles with relative long duration

(respectively, Ap3 and Ap5 of Jacquin et al., 1998; Figure 8), instead of to sea-level lowstands (Morgan, 1980b). The present study also shows that in the progressively marine character of the upper Yappar Member in combination with the Coffin Hill Member corresponding to Aptian rather than to Barremian, only one pre-Aptian transgressive phase can be recognized, and not two.

The correlation of the inferred sea-level signature for Mossman with the latest Barremian-Aptian eustatic sea-level curve of Hardenbol et al. (1998) and Jacquin et al. (1998) is also confirmed by the chemostratigraphic recognition of the global organic-carbon-isotope segments C2 to C10 (defined by Menegatti et al., 1998 and Bralower et al., 1999; Figure 6). Based on the isotope segments, the precise stratigraphic correlation for the top of the studied section remains problematic, but segments C11 and C12 are probably contained and a Late Aptian age seems most plausible.

During the past few years a wealth of information on carbon-isotope data on the Upper Barremian-Aptian became available, mainly in relation to the recognition of OAE 1a in other than deeper marine settings (e.g. de Gea et al., 2003; Gröcke et al., 1999; Heimhofer et al., 2003; Vilas et al., 2003; Wissler et al., 2002). According to Menegatti et al. (1998) and Bralower et al. (1999) the Lower Aptian OAE 1a starts with a marked increase in global  $\delta^{13}\text{C}_{\text{org}}$  values, comprising segments C4 to C6 (see Figure 4). In the Cismon section OAE 1a starts approximately 500 Kyr years after the Aptian boundary (Herbert, 1992; Erba et al., 1999). Although these authors inferred a different duration for OAE 1a (i.e., for 5 meters of core containing the Selli Level Herbert (1992) inferred 1.2 My and Erba et al. (1999) 450 Kyr), both numbers infer extremely short times for the two 3<sup>rd</sup> order eustatic sea-level cycles Ap1 and Ap2 (Hardenbol et al., 1998; Jacquin et al., 1998), being in the order of parasequences and/or Milankovitch cyclicity (Herbert, 1992).

The series of deep earliest Aptian sea-level drops of Ap1, Ap2, with sequence boundary Ap3 as climax, is considered to have been responsible for the global nutrification event ("Nannoconid crisis," as proposed by Erba, 1994 and Larson and Erba, 1999) preceding OAE 1a. The stratigraphic position of the "nannoconid crisis" seems to vary in sequences from different deposition basins, i.e. it has been observed prior to, during, and/or after magnetic Polarity Chron M0 (as indicated in, e.g. Bralower et al., 1994, 1999). The exact position of the "nannoconid crisis" probably depends on the particular palaeoenvironmental setting and architecture of the different basins.

The sea-level drops related with Ap1 to Ap3 might further have led to hiatuses within the sandstone deposits in this interval in Mossman. This could probably obscure the extreme negative  $\delta^{13}\text{C}_{\text{org}}$  values characteristic for the Aptian boundary (see Erba et al., 1999) and possibly explain why isotope segment C3 is not truly expressed in Mossman.

The return to relatively high sea-level in the Early Aptian is generally believed to be the result of global warming due to intense volcanic  $\text{CO}_2$  outgassing during construction of the Ontong Java Plateau and Nova Canton Trough (e.g. Larson, 1991; Larson and Erba, 1999) with superimposed, extremely rapid release of methane hydrates into the ocean and atmosphere (Hesselbo et al., 2000; Weissert, 2000; Jahren et al., 2001), which resulted in the strong negative excursion of organic-carbon-isotope segment C3 (Wissler et al., 2002).

The following strong positive shift in global  $\delta^{13}\text{C}_{\text{org}}$  values of segments C4 to C6, related to OAE 1a, lie within the Transgressive Systems Tract (Bralower et al., 1999) and from Mossman it is inferred to correspond with the TST of cycle Ap3 (Haq et al., 1987 ; Hardenbol, 1998; Figure 8). Another consequence of global warming is increased humidity due to enhancement of the hydrological cycle (Menegatti et al., 1998). In Mossman relative wet and warm conditions occur prior to OAE 1a (Figure 7, segment 2), but for the time of the inferred excess input of  $\text{CO}_2$  due to the oxidation of methane hydrates no obvious palaeoenvironmental change is apparent. Most obvious changes in Mossman seem to occur from the presumed onset of OAE 1a, at the start of segment C4, when circumstances suddenly become drier and cooler (see also Menegatti et al., 1998; Hochuli et al., 1999; Price, 2003; Figure 3 and 7). These conditions might be related to a

circum-Antarctic-Australian current system inferred to develop in the Early Cretaceous (Baumgartner et al., 1992; Chapter 2), which would bring relatively cooler waters to northeastern Australia.

In pelagic successions black-shale intervals related with OAE 1a correspond to high TOC-values in sediments (e.g. Menegatti et al., 1998; Bralower et al., 1999; Leckie et al., 2002; Price, 2003). To explain the occurrence of widespread anoxia two contrasting models were postulated. In the first, preservation is improved due to oxygen depletion (e.g. Schlanger and Jenkyns, 1976; De Boer, 1986). The dysoxic or anoxic conditions created at the seafloor are caused by an enhanced stratification of the water column and result in better preservation of organic matter (e.g. Bralower and Thierstein, 1984). The second model is a high productivity model (e.g. Pederson and Calvert, 1990). This model requires sufficient ventilation and nutrient recycling. Due to enhanced primary productivity more oxygen is consumed during sedimentation of the organic matter, eventually leading to a surplus in organic matter, which is stored in the sediment (e.g. Pederson and Calvert, 1990; Hochuli et al., 1999). In Mossman a 1.5m thick, gray mudstone and shale corresponding with isotope segment C5 (Figure 8) could be regarded as an equivalent of the black shale generally related with OAE 1a. In this interval in Mossman a minor peak in dinocyst productivity (P/G ratio) is apparent which might support the high productivity conditions but conclusive evidence is lacking since the TOC-values are not extreme (Figure 3 and 4, segment C5). These moderate values are probably due to the relatively shallow marine setting in which most of the organic carbon formed could be oxidized again.

In general, high global TOC-values coincide with positive excursions in the global  $\delta^{13}\text{C}_{\text{org}}$  record, reflecting periods of excess organic carbon stored in black shales (e.g. Weissert, 1989; Bralower, 1994, 1999; Menegatti et al., 1998; Price 2003). The burial of organic matter leads to a decrease of the greenhouse gas  $\text{CO}_2$ , which in turn will lead to global cooling (e.g. Bralower 1994; Leckie et al., 2002; Price, 2003). In Mossman-1 intervals with increasing  $\delta^{13}\text{C}_{\text{org}}$  values are paralleled by high frequencies of cool/temperate dinocysts (Figure 4) but interestingly the culmination of these dinocysts lies at the base of the shale inferred to relate to OAE 1a. The incursion of the cool/temperate dinocysts at Mossman-1 therefore seems to be related to the earliest Aptian sea-level rise of cycle T13 rather than to a cooling effect due to excess burial of organic matter. This sea-level rise probably enabled encirclement of the Antarctic-Australian landmass by cool water-currents.

Within the Late Aptian other possible oceanic anoxic events have been observed (Breheret, 1988; Weissert and Breheret, 1991; Bralower et al., 1999; Herrle et al., 2004). According to Bralower et al. (1999) the event in the middle Late Aptian correlates to the transition between isotope segment C8 and C9 (indicated in Figure 6, La Boca Canyon section). These authors documented this positive excursion in their  $\delta^{13}\text{C}_{\text{org}}$  record to correspond with high TOC-values. Bralower et al. (1999) further note that this possible OAE was observed in vicinity of a sequence boundary. From Mossman it is clear that the transition between segments C8 and C9 falls within the Ap4 sequence (Hardenbol et al., 1998; Jacquin et al., 1998; Figure 8) but TOC-values do not indicate the presence of a possible OAE equivalent and the global extent of this questionable OAE remains uncertain.

## Conclusions

Based on biostratigraphic correlation of dinoflagellate cyst events the investigated interval of well BMR Mossman-1 (15.32-159.05 m in core) corresponds to uppermost Barremian-Aptian. By absence of appropriate biomarkers the stratigraphy of the top of the interval could not be assessed

properly, but most probably corresponds to Upper Aptian. This is confirmed by the resemblance of the inferred sea-level signature for Mossman and the eustatic sea-level curve of Hardenbol et al. (1998) and Jacquin et al. (1998) of which all 2<sup>nd</sup> order transgression-regression fluctuations and all 3<sup>rd</sup> order variations for the latest Barremian-Aptian could be identified (cycles Ba6 and Ap1 to Ap5). Moreover, all latest Barremian-Aptian global organic-carbon-isotope segments defined by Menegatti et al. (1998) and Bralower et al. (1999) could be identified in the  $\delta^{13}\text{C}_{\text{org}}$  curve for the studied interval from Mossman.

Analysis of the sporomorph data led to determination of the vegetation history of the coastal plain area from where the Mossman sediments were derived. Evaluation of the integrated palynological results permitted detailed reconstruction of the progressive development of the local environmental conditions at Mossman.

Comparison of the organic-carbon-isotope stratigraphy from Mossman with Tethyan and Boreal sequences revealed that these curves are essentially identical. Apart from isotope segment C3, which falls within a sandy interval likely to contain several hiatuses related with sequence boundaries Ap1 to Ap3, the isotope segments show a similar pattern with approximately the same magnitude. The global carbon isotope segments C4-C6 in Mossman correspond with the transgressive systems tract of the Ap3 sequence, during which the probable equivalent of the black shale related to OAE 1a was deposited. In Mossman this interval correlates with a 1.5 m thick, gray shale and mudstone and corresponds with isotope segment C5. Although, this unit is associated with an increase in productivity and significant environmental changes associated with an OAE event do occur, the interval does not show elevated TOC values.

In Mossman, intervals of increased  $\delta^{13}\text{C}_{\text{org}}$  values are paralleled by high amounts of cool/temperate dinocysts. The FO of *C. granulatum* is possibly related to these cooler conditions, instead of occurring in the uppermost Barremian, it shows a delayed first occurrence in the Lower Aptian. This change to cool water conditions is coeval with the rapid sea-level rise of the Ap3 sequence, and might indicate that a circum-Antarctic-Australian connection existed in the Early Aptian.

The  $\delta^{13}\text{C}_{\text{org}}$  records for the middle Late Aptian interval possibly containing an oceanic anoxic event, and correlates to the transition between isotope segment C8 and C9, show similar patterns in shape and magnitude. However, TOC-values from Mossman-1 do not indicate the presence of a possible OAE equivalent. The transition between segments C8 and C9 in Mossman falls within the Ap4 stratigraphic sequence.

The bio- and chemostratigraphy in combination with the inferred sea-level fluctuations enabled verification and refinement of the ages of the lithostratigraphical units identified in the studied interval at Mossman. The Yappar Member is of latest Barremian-earliest Aptian age, the entire Coffin Hill Member is exclusively earliest Aptian, and the Wallumbilla Formation in Mossman is Aptian in age. The present study shows that the lithological boundaries (Gilbert River Formation-Wallumbilla Formation and Yappar Member-Coffin Hill Member) represent progressive steps to more open marine facies. These boundaries are inferred to correspond to eustatic Transgressive Systems Tracts of cycles with relative long duration.

The present study infers a shallow marine depositional palaeoenvironment for the upper part of the Yappar Member, rather than being exclusively of fluvial origin.

Within the lithological units from Mossman four of the dinoflagellate zones from the Australian Mesozoic zonation scheme were recognized; in ascending order these are: *M. australis* Zone, *O. cinctum* Zone, *O. operculata* Zone, and *D. davidii* Zone. Two sporomorph zones are identified: *Foraminisporis wonthaggiensis* and *Cyclosporites hughesii*.

In terms of standard stratigraphy, the *O. cinctum* Zone correlates to the *tuarkyricus* and lower *weissi* ammonite Chronozones. In Mossman the FO of *T. tenuiceras* lies within the acme zone, confirming its position within the *tuarkyricus* ammonite Chronozone.

The Barremain-Aptian boundary lies in the latest *M. australis* Zone. The inferred *D. davidii* Zone occurs at the top of the Mossman section and corresponds to sequence boundary Ap6, which approximates the Albian boundary. Consequently, the entire *O. cinctum* Zone, the successive *O. operculata* Zone, and the lowermost *D. davidii* Zone are Aptian. Based on the calibrated levels in Australia the *F. wonthaggiensis* sporomorph Zone correlates with Barremian-lowermost Aptian and the succeeding *C. hughesii* sporomorph zone with the Aptian.

## Dinoflagellate cyst species list and taxonomic remarks for BMR Mossman-1

### List of identified taxa

For documentation of the taxa identified in the present study, see the Lentin and Williams Index (Williams *et al.*, 1998). A selection of taxa is illustrated in Plates 1 and 2 where sample codes, preparation slide numbers, size of the specimens and England Finder Co-ordinates (EFC) are indicated. For remarks on taxa encountered in Mossman-1 as well as in Angles and/or DSDP site 263 is referred to the taxonomical section in chapter 2.

The listed numbers refer to the order in the distribution data in Table 3.

	Table 3	Plate 1	Plate 2
<i>Acanthaulax</i> sp.A	59		
<i>Achomosphaera</i> spp	57		
<i>Adnatosphaeridium chonetum</i>	72		
<i>Angustodinium acribes</i>	73	1k	
<i>Aprobolocysta eilema</i>	64		
<i>Aprobolocysta</i> sp.A	62		
<i>Apteodinium granulatum</i>	17		
<i>Apteodinium maculatum</i>	31		
<i>Apteodinium</i> spp	58		
<i>Batiacasphaera</i> spp	66		
<i>Batioladinium jaegeri</i>	43		
<i>Batioladinium micropodum</i>	38		
<i>Canningia</i> cf. sp. <i>C. transitoria</i>	36		2g
<i>Canningia reticulata</i>	50		2h, 2i
<i>Canningia</i> sp.A (Morgan)	79		
<i>Canningia transitoria</i>	24		2e, 2f
<i>Cannosphaeropsis/Hapsocysta</i>	74		2k-m
<i>Carpodinium granulatum</i>	70	1h	
<i>Cassiculosphaeridia reticulata</i>	16		
<i>Chlamydophorella</i> spp	10		
<i>Circulodinium colliveri</i>	26		
<i>Cleistosphaeridium</i> spp	3		
<i>Cometodinium</i> spp	55		
<i>Coronifera oceanica</i>	27		
<i>Cribroperidinium</i> spp	6		
<i>Cyclonephelium</i> spp	14		
<i>Dapsilidinium</i> spp	18		
<i>Dapsilidinium warrenii</i>	75		

	Table 3	Plate 1	Plate 2
<i>Diconodinium davidii</i>	85	1p	
<i>Diconodinium</i> spp	83		
<i>Dingodinium cerviculum</i>	1		
<i>Discordia nanna</i>	41		
<i>Elytrocysta circulata</i>	28		
<i>Endoceratium polymorphum</i>	84		2a-d
<i>Endoscrinium bessebae</i>	65		2j
<i>Endoscrinium campanula</i>	68		
<i>Epitricysta vinckensis</i>	47	1j	
<i>Exocho-/Pervosphaeridium</i> spp	5		
<i>Fibradinium variculum</i>	80	1l	
<i>Florentinia</i> spp	23		
<i>Fromea</i> cf. <i>F. amphora</i>	77		
<i>Fromea monolifera</i>	45		
<i>Gonyaulacysta</i> spp	48		
<i>Heslertonia</i> spp	81		
<i>Hystrichodinium pulchrum/voigtii</i>	37		
<i>Hystrichodinium</i> spp	56		
<i>Impagidinium</i> spp	63		
<i>Kallosphaeridium</i> spp	7		
<i>Kleithriasphaeridium eoinodes</i>	22		
<i>Kleithriasphaeridium</i> spp	33		
<i>Leiasphaera</i> spp	19		
<i>Leptodinium hyalodermopsis</i>	76		
<i>Leptodinium</i> spp	82		
<i>Lithodinia helbyi</i>	44		
<i>Lithodinia</i> spp	61		
<i>Lithodinia stoveri</i>	60		
<i>Muderongia australis</i>	21	1i	
<i>Muderongia crucis</i>	39		
<i>Muderongia mcwhaei</i>	69	1n	
<i>Muderongia</i> sp. cf. <i>M. staurota</i>	34		
<i>Muderongia</i> spp	29		
<i>Muderongia tetracantha</i>	42		
<i>Occisucysta</i> spp	49		
<i>Odontochitina operculata</i>	67	1g	
<i>Oligosphaeridium</i> cpx.	4		
<i>Ovoidinium cinctum</i>	40	1o	
<i>Paleoperidinium cretaceum</i>	52		
<i>Pareodinia ceratophora</i>	15		
<i>Platycystidia eisenackii</i>	46		
<i>Prolixosphaeridium parvispinum</i>	30		
<i>Rhombodella natans</i>	11		
<i>Rigaudella/Adnatosphaeridium?</i>	25		
<i>Scriniodinium attadalense</i>	35		
<i>Sentusidinium</i> spp	2		
<i>Spinidinium boydii</i>	86	1m	
<i>Spiniferites</i> spp	8		
<i>Stiphrosphaeridium anthophorum</i>	20		
<i>Tanyosphaeridium</i> spp	12		

	Table 3	Plate 1	Plate 2
<i>Tehamadinium sousensis</i>	32	1d, 1e	
<i>Tehamadinium</i> spp	78		
<i>Tehamadinium tenuiceras</i>	53	1a-c	
<i>Tetrachacysta allenii</i>	51		
<i>Trichodinium</i> spp	9		
<i>Valensiella magna</i>	54	1f	
<i>Walloadinium lunum</i>	13		
<i>Yalkalpodium scutum</i>	71		

### *Taxonomic remarks*

#### *Endoceratium polymorphum*

Specimens assigned to this taxon exhibit a dense intratabular reticulum consisting of spinose ornamentation with fused, discontinuous crests. Seemingly differing from the tabular ornamentation of *E. turneri*.

Morgan (1980) reported that his Australian specimens of *E. polymorphum* are relatively rounded. However, the specimens encountered in Mossman-1 are subrounded to square and possess clearly developed lateral and antapical horns and resemble specimens from the Tethyan realm as described by Davey and Verdier (1974).

#### *Exocho-/Pervosphaeridium* spp

It was not possible to discern the archeopyle for most specimens and these were therefore put in the one group.

## Plate 5

Light photomicrographs of key dinocyst taxa at BMR Mossman-1.

- a, *Tehamadinium tenuiceras*, body width 63  $\mu\text{m}$ , sample 127.27 m EFC J25.
- b, idem, body width 67  $\mu\text{m}$ , sample 114.45 m EFC B35.
- c, idem, body width 70  $\mu\text{m}$ , sample 121.96 m EFC D52.
  
- d, *Tehamadinium sousensis*, body width 61  $\mu\text{m}$ , sample 155.52 m EFC Q31.
- e, idem, body width 72  $\mu\text{m}$ , sample 132.52 m EFC A31/3.
  
- f, *Valensiella magna*, body width 89  $\mu\text{m}$ , sample 125.49 m EFC C36.
  
- g, *Odontochitina operculata*, body width 45  $\mu\text{m}$ , sample 117.01 m EFC D48/1.
  
- h, *Carpodinium granulatum*, body width 32  $\mu\text{m}$ , sample 114.46 m EFC U17/2.
  
- i, *Muderongia australis*, body width 50  $\mu\text{m}$ , sample 155.52 m EFC H35/2.
  
- j, *Epitricysta vinckensis*, 46  $\mu\text{m}$ , sample 137.06 m EFC U36.
  
- k, *Angustodinium acribes*, width cingulum 24  $\mu\text{m}$ , sample 16-1 EFC N42/2.
  
- l, *Fibradinium* spp, total width 32  $\mu\text{m}$ , sample 15-1 EFC H44/1.
  
- m, *Spinidinium boydii*, width 30  $\mu\text{m}$ , sample 15.32 m EFC S32.
  
- n, *Muderongia mcwhaei*, inner body width 62  $\mu\text{m}$ , sample 114.45 m EFC U34/1.
  
- o, *Ovoidinium cictum*, width 53  $\mu\text{m}$ , sample 127.27 m EFC J48.
  
- p, *Diconodinium davidii*, width 56  $\mu\text{m}$ , sample 15.32 m EFC N31/4.

Plate 5

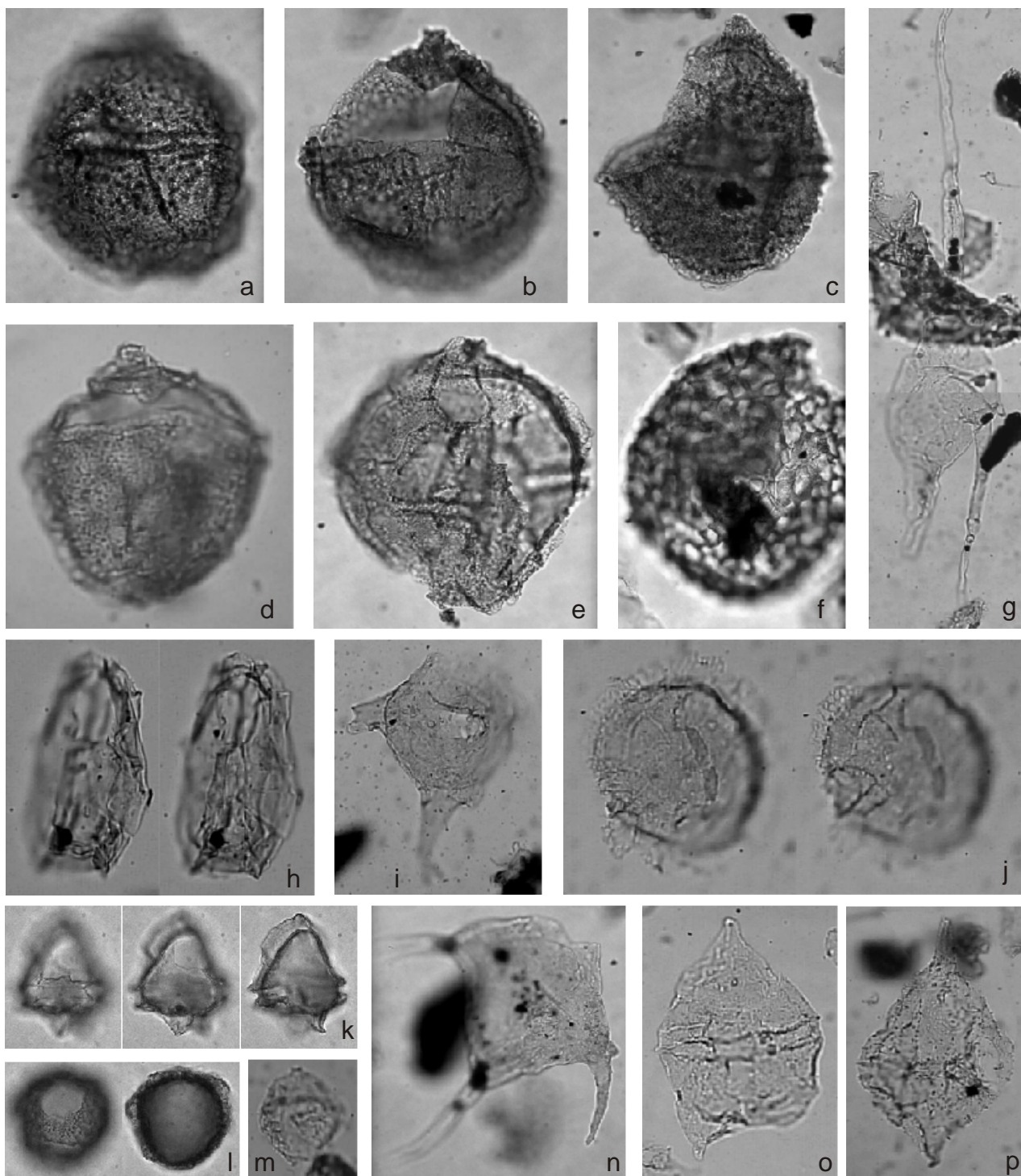


## Plate 6

Light photomicrographs of key dinocyst taxa at BMR Mossman-1.

a, b, c, d, *Endoceratium polymorphum*, body width 100  $\mu\text{m}$ , sample 15.32m EFC H47/1.

e, f, *Canningia transitoria*, inner body width 76  $\mu\text{m}$ , sample 159.05m EFC Q22/3.

g, *Canningia* cf. sp. *C. transitoria*, inner body 82  $\mu\text{m}$ , sample '151.08m' EFC E38/1.

h, *Canningia reticulata*, body width  $\sim 95$   $\mu\text{m}$ , sample 117.01m EFC A34/3.

i, idem, body width  $\sim 90$   $\mu\text{m}$ , sample 117.01m EFC R49/3.

j, *Endoscrinium bessebae*, width central body  $\sim 42$   $\mu\text{m}$ , sample 114.45 m (30-1) EFC V45/2.

k, l, m, *Cannosphaeropsis australis*, width central body 46  $\mu\text{m}$ , sample 117.01 m (34-1) EFC M49/4.

Plate 6

